AN EXPERIMENTAL STUDY ON THE PERFORMANCE OF GEOTEXTILE TUBES IN BEACH NOURISHMENT APPLICATIONS

A THESIS SUBMITTED TO
THE GRADUATE SCHOOL OF NATURAL AND APPLIED SCIENCES
OF
MIDDLE EAST TECHNICAL UNIVERSITY

BY

EMRECAN IŞIK

IN PARTIAL FULFILLMENT OF THE REQUIREMENTS
FOR
THE DEGREE OF MASTER OF SCIENCE
IN
CIVIL ENGINEERING

AUGUST 2019

Approval of the thesis:

AN EXPERIMENTAL STUDY ON THE PERFORMANCE OF GEOTEXTILE TUBES IN BEACH NOURISHMENT APPLICATIONS

submitted by **EMRECAN IŞIK** in partial fulfillment of the requirements for the degree of **Master of Science in Civil Engineering Department, Middle East Technical University** by,

Prof. Dr. Halil Kalıpçılar
Dean, Graduate School of **Natural and Applied Sciences** ________________

Prof. Dr. Ahmet Türer
Head of Department, **Civil Engineering** ________________

Assist. Prof. Dr. Cüneyt Baykal
Supervisor, **Civil Engineering, METU** ________________

Examining Committee Members:

Prof. Dr. Ahmet Cevdet Yalçıner
Civil Engineering, METU ________________

Assist. Prof. Dr. Cüneyt Baykal
Civil Engineering, METU ________________

Prof. Dr. Mehmet Ali Kökpınar
Civil Engineering, TED University ________________

Assist. Prof. Dr. Gülizar Özyurt Tarakcıoğlu
Civil Engineering, METU ________________

Assist. Prof. Dr. Alp Küçükosmanoğlu
Civil Engineering, Mehmet Akif Ersoy University ________________

Date: 29.08.2019

I hereby declare that all information in this document has been obtained and presented in accordance with academic rules and ethical conduct. I also declare that, as required by these rules and conduct, I have fully cited and referenced all material and results that are not original to this work.

Name, Surname: Emrecan Işık

Signature:

ABSTRACT

AN EXPERIMENTAL STUDY ON THE PERFORMANCE OF GEOTEXTILE TUBES IN BEACH NOURISHMENT APPLICATIONS

Işık, Emrecan
Master of Science, Civil Engineering
Supervisor: Assist. Prof. Dr. Cüneyt Baykal

August 2019, 86 pages

In this study, performance of submerged geotextile tubes as toe protection for the beach nourishment applications was investigated through physical model tests. Cross-shore sediment transport volumes and sand protection performances of geotextile tubes were evaluated based on the measured post-storm beach profile changes and recessions or progressions of shoreline. In the experiments, the effects of fill material sediment grain sizes, fill angles, negative freeboards of geotextile tubes, and wave steepnesses were investigated. According to the profile measurements, the increase in the significant wave height and wave steepness were found as augmentative factors of beach erosion. It was observed that the increase in sand grain diameter reduces the sediment movement in nearshore, while steepening of the fill angle strengthened the effect of the erosive and accretive waves. It was also observed that using tubes as toe protection in beach nourishment applications in wave breaking zone did not have positive effects on recessions or progressions, instead geotextile tubes placed outside of breaking zone as submerged breakwaters worked more efficient.

Keywords: Beach Nourishment, Geotextile Tube, Sediment Transport, Coastal Morphology, Accretive/Erosive Waves

ÖZ

KIYI BESLEMESİ UYGULAMALARINDA JEOTEKSTİL TÜPLERİN PERFORMANSI ÜZERİNE DENEYSEL BİR ÇALIŞMA

Işık, Emrecan
Yüksek Lisans, İnşaat Mühendisliği
Tez Danışmanı: Dr. Öğr. Üyesi Cüneyt Baykal

Ağustos 2019, 86 sayfa

Bu çalışmada batık jeotekstil yapıların kıyı besleme uygulamalarında topuk koruma olarak performansları fiziksel model deneyleriyle araştırılmıştır. Kıyıya dik sediman taşınım miktarları ve jeotekstil tüplerin kum tutma performansları uygulanan besleme profillerindeki fırtına sonrası değişimlere (erozyon ve birikme) ve kıyı çizgisindeki geri çekilme ya da ilerleme mesafelerine göre değerlendirilmiştir. Deneylerde sediman tane boyutu, besleme eğimi, jeotekstil tüplerin su kesimleri ve dalga diklikleri değişken tutulmuştur. Taban profilindeki ve kıyı çizgisindeki değişimler incelendiğinde, belirgin dalga yüksekliğinin ve dalga dikliğinin artması aşınma miktarını artıran etmenler olarak görülmüştür. Kum tane çapının artmasının yakın kıyıdaki sediman hareketini azalttığı, besleme açısının dikleşmesinin aşındıran ve biriktiren dalgaların özelliklerini güçlendirdiği gözlemlenmiştir. Kıyı beslemesiyle birlikte kırılma bölgesinde topuk yapısı kullanımının geri çekilme ve ilerlemelere olumlu bir etkisi olmadığı, kırılma bölgesinin dışına yerleştirilen jeotekstil tüplerin ise batık dalgakıran olarak daha verimli çalıştığı görülmüştür.

Anahtar Kelimeler: Kıyı Beslemesi, Jeotekstil Tüp, Sediman Taşınımı, Kıyı Morfolojisi, Biriktiren/Aşındıran Dalgalar

to my beloved family and friends,

ACKNOWLEDGEMENTS

First and foremost, I have to thank my beloved family for their unconditional support throughout my life. They always respect my decisions and do what is necessary to accomplish my future goals.

I would like to express my deepest gratitude to my supervisor, Assist. Prof. Dr. Cüneyt Baykal about everything he taught me from the beginning of my journey to becoming a coastal engineer. He has led me, guided me, helped me and worked with me for the last three and a half years. His contributions to my thesis, my career and life are so valuable that I hope our studies together will continue even though my master's degree will be completed.

My special thanks are for my second family, Coastal and Ocean Engineering Laboratory. Especially, Prof. Dr. Ahmet Cevdet Yalçıner has come to my rescue whenever I needed. He has not only provided me an opportunity that worked as a project assistant at the laboratory, but also helped me to choose elective coastal engineering classes in my senior year. That is why I have been able to know Prof. Dr. Ayşen Ergin and Assist. Prof. Dr. Gülizar Özyurt Tarakcıoğlu when I was an undergraduate student. Their passion and motivation for teaching and coastal engineering have enlightened me to pursue my career path.

I would like to sincerely thank Assist. Prof. Dr. Işıkhan Güler, both my teacher/advisor and my employer. Besides his experience about the subject have always been useful, he has encouraged me do my best and shared his opinions while I was finishing the thesis study. I also would like to thank my boss, Yasemin Özgen and all co-workers for their understanding about my flexible working schedule.

I would like to thank our laboratory staff, secretary Nuray Sefa, who is expert in documentation, and technician Yusuf Korkut, who has made great efforts in setting up the physical model experiment, preparing the wave channel and necessary equipment.

My special thanks are for H. Gökhan Güler, both my wave channel and military buddy, Koray D. Göral, who has assisted me in conducting the experiments and carrying out the measurements, Cem Bingöl, M. Efekan Çevik, M. Sedat Gözlet, Cansu Balku, Ecemnur Aydın and Bora Yalçıner for their physical, technical and mental supports throughout the experiment and thesis writing processes.

I would like to thank my colleagues, classmates and dearest friends Duha Metin, G. Ezgi Çınar, İzel Akdeniz, Arif Uğurlu, Çağıl Kirezci, Ghazal Khodkar, Can Özsoy, Kadir Karakaş, G. Güney Doğan and Ebru Demirci for everything we share and guidance of their own studies.

I would like to express my gratitude to METU Ocean Engineering Research Center for the use of laboratory equipment and financing the necessary materials. I also would like to thank Construction Materials Laboratory technician Cuma Yıldırım about the tests he carried out for my study, and finally, TenCate Geosynthetics representatives Serhan Akın, Emre Aka and Mink ter Harmsel for providing geotextile materials, books and brochures.

TABLE OF CONTENTS

LIST OF TABLES

TABLES

LIST OF FIGURES

FIGURES

LIST OF ABBREVIATIONS

ABBREVIATIONS

2DH	Two Dimensions in Horizontal
3D	Three-Dimensional
AFS	American Foundry Society
ASTM	American Society for Testing and Materials
CUR	Centre for Urban Research and Land Development
DHI	Danish Hydraulic Institute
GENESIS	Generalized Model for Simulating Shoreline
IAHR	International Association for Hydraulic Research
MATLAB	Matrix Laboratory
METU	Middle East Technical University
MWL	Mean Water Level
OERC	Ocean Engineering Research Center
PIANC	Permanent International Association of Navigation Congresses
SPM	Shore Protection Manual
SWL	Still Water Level
TDG	Test Data Generator
TMA	Texel-Marsen-Arsloe
TS	Turkish Standards

LIST OF SYMBOLS

SYMBOLS

A	Sediment-dependent shape (scale) parameter
B	Berm height of beach
C_D	Drag coefficient
D	Grain diameter of sediment
D_{50}	Median grain diameter of sediment
Fr	Froude number
H	Wave height
H_{m0}	Significant wave height (from spectrum)
H_{max}	Maximum wave height
H_s	Significant wave height
$H_{s,12}$	Significant wave height that 12 hours per year
L	Wavelength
L_0	Deep-sea wavelength
L_m	Model length
L_p	Prototype length
N	Number of waves
R_C	Crest depth
Re	Reynolds number

S	Wave set-up
S_0	Stroke amplitude of piston
SG	Specific gravity
T	Wave period
T_m	Mean wave period
$T_{m,-10}$	Spectral wave period
T_s	Significant wave period
T_p	Peak wave period
V_D	Volume of deposition/accretion
V_E	Volume of erosion
W	Berm width of beach nourishment
W_*	Width up to closure depth
W_e	Shoreline progression width
b	Base width of geotextile tube
b_t	Maximum width of geotextile tube
d	Depth of water
d_c	Closure depth
d_t	Toe depth of geotextile tube
f	Frequency
g	Gravitational acceleration
h	Depth of water

h_*	Closure depth
h_t	Height of geotextile tube
k	Wave number
m	Bottom slope
s	Wave steepness
u	Flow velocity
w_s	Sediment fall (settling) velocity
y	Cross-shore distance
Δy	Recession/progression distance
Π	Nondimensional parameter
Ω	Gourlay parameter
α	Fill angle
γ	Unit weight
η	Surface elevation
λ_L	Length scale
λ_T	Time scale
μ	Dynamic viscosity
υ	Kinematic viscosity
π	Dimensional parameter
ρ	Density
σ_v'	Average vertical stress

CHAPTER 1

INTRODUCTION

“Beaches provide a wide range of societal benefits including storm protection, recreation, and habitat for a number of species. However, many beaches are under natural and/or human induced erosional pressures” (Dean, 2005, p. 25). To overcome this problem, coastal engineers or designers have a few options like retreating from the shoreline, correcting the human related erosional cause, armoring the shore or nourishing the beach. Although beach nourishment is the most practical, feasible and environment friendly application among them, it must be repeated every 2 years unless it is protected against wave attack (Dean, 2002).

For shoreline restoration and protection applications, geotextile sand containers have been increasingly popular over the recent years. Compared to rubble mound structures, geotextile based soft structures provide flexibility in field applications, such as easy removal or relocation of the structure based on its performance by emptying the containers via pumping out the sand. As a result, number of perched beaches with geotextile tubes used as a toe structure of beach nourishment has risen over the years.

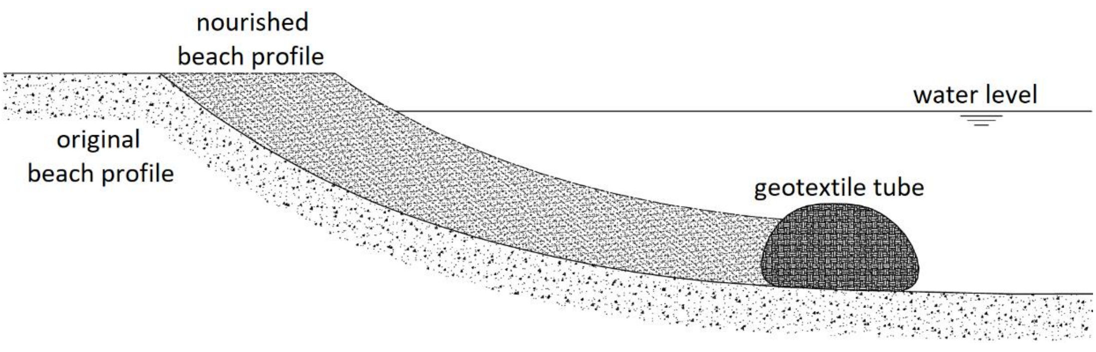

Figure 1.1. Cross-Section of Beach Nourishment Application with a Toe Structure

In this study, performance of submerged geotextile tubes as a toe protection for the beach nourishment applications is investigated through physical model experiments based on the measured post-storm beach profile changes, recessions or progressions of shoreline and erosion or accretion rates. At the end of the study, it is aimed to find appropriate answers to following questions; (i) can both erosive and accretive waves be modeled in laboratory environment? (ii) how does changing wave parameters affect the post-storm bottom profiles? (iii) does the sediment grain size have a critical role on recession/progression? (iv) what are the effects of fill angle in beach nourishment applications? (v) what are the ideal sizes and depths of geotextile tubes? (vi) do geotextile tubes become successful being used as a toe or a submerged breakwater?

In chapter two, general background information about cross-shore sediment transport, beach nourishment applications, shoreline protection systems and the area of use for geotextile materials are given to explicate the main concept of the study. In addition, previous studies of both physical and numerical model experiments about the subject, the use of geotextile sand containers in coastal protection applications, are surveyed and summarized as a literature review.

In chapter three, the methodology, instrumentation, model scale, experimental setup, profile measurement and data post-processing are described in detail.

In chapter four, results of physical model experiments are given. First, wave calibration experiments were carried out, then winter and summer storms are generated by using different wave parameters. The post-storm beach profiles are presented comparatively. For the next step, effects of different parameters are investigated. These parameters listed as sand grain sizes, beach fill slopes, toe and crest depths of geotextile tubes and finally the presence of toe structure. Beach erosion and accretion distances are measured in order to make provisions about the effects of beach nourishment parameters.

In chapter five, the study is summarized, conclusions, discussion of results and future recommendations are given for the continuum of the study.

CHAPTER 2

LITERATURE REVIEW

Shore protection is always one of the most critical tasks for coastal engineering. There is a significant amount of work about beach erosion due to waves in the literature.

As a background information about the concept, coastal definitions (Figure 2.1) and a statement given in Shore Protection Manual (US Army, Corps of Engineers, 1984) is presented: “Where the land meets the ocean at a sandy beach, the shore has natural defenses against attack by waves, currents and storms. The first of these defenses is the sloping nearshore bottom that causes waves to break offshore…” (p. 3).

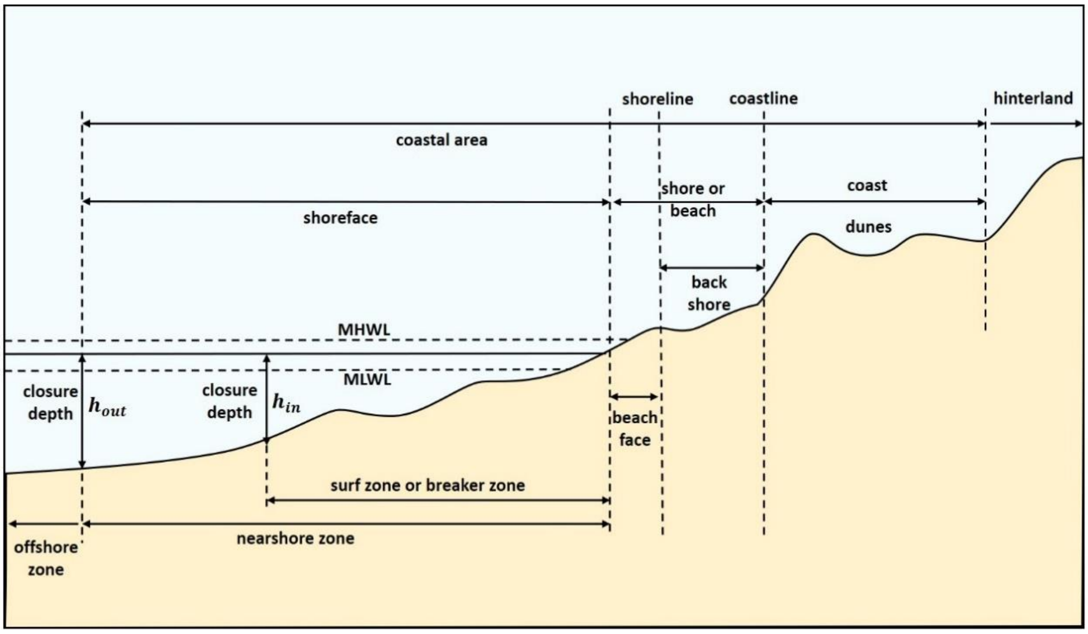

Figure 2.1. Definitional Sketch of a Typical Beach Profile (Adapted from SPM, 1984)

In this chapter, previous studies regarding to cross-shore sediment transport, shoreline protection, beach nourishment, geosystems and model experiments are reviewed.

2.1. Cross-Shore Sediment Transport

Equilibrium beach profiles due to sand properties, and post-storm erosion/accretion solely depends on wave parameters are the two major headlines of the topic.

Dean (1991) stated four features of equilibrium beach profiles. They tend to concave upwards, larger sediment diameters are associated with steeper slopes, the beach face is approximately planar and finally, steep waves have a tendency for bar formation.

Bruun (1954) suggested a formula after analyzing beach profiles from Mission Bay, California and Danish North Sea Coast as Dean (1977) approved using least squares:

$$h(y) = Ay^{2/3} \qquad \text{Eq. 2.1}$$

where h is the depth of water, y is the cross-shore distance and A is the sediment-dependent shape parameter. Moore (1982) suggested an empirical relationship between shape parameter and sediment diameter, D (Figure 2.2).

After combining and analyzing the results of tank and field experiments that Swart (1974), Moore (1982) and Hughes (1983) carried out, Dean (1987) stated that the shape parameter does not only depend on sediment diameter; it can be related to the fall velocity of the sediment, w_s. (Eq. 2.2).

$$A = 0.067\, {w_s}^{0.44} \qquad \text{Eq. 2.2}$$

Fall velocity equation that derived by Stokes (1851) is given in Eq. 2.3:

$$w_s = \frac{gD^2(\rho_s - \rho_w)}{18\mu} \qquad \text{Eq. 2.3}$$

where g is the gravitational acceleration, ρ_s is the density of sediment, ρ_w is the density of water (fluid) and μ is the dynamic viscosity of the water (fluid).

Then, "A vs D curve" was transformed using fall velocity relationship and presented in Figure 2.2.

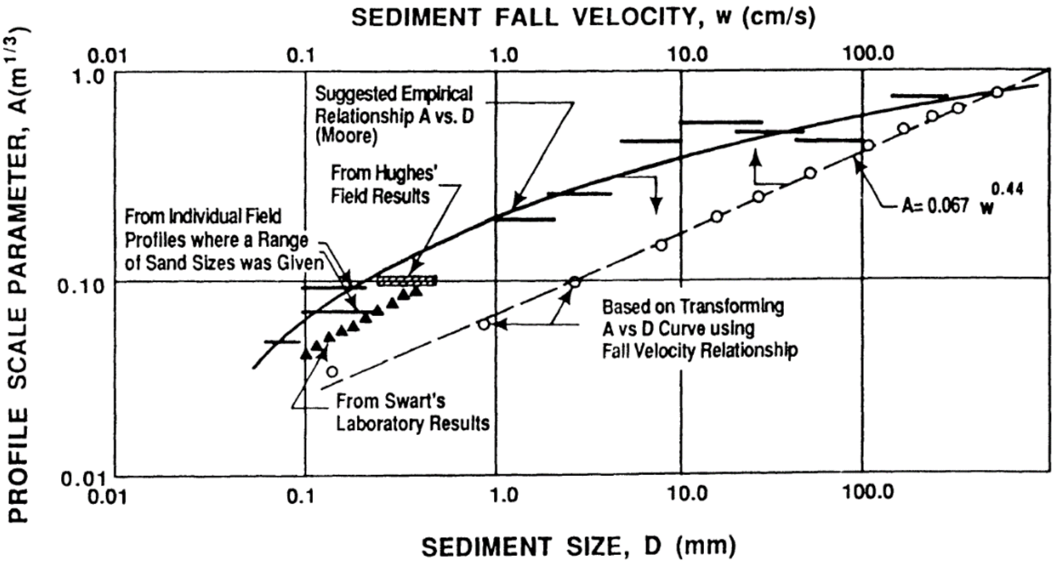

Figure 2.2. Beach Profile Scale Parameter (A) vs Sediment Diameter (D) and Fall Velocity (w_s) (Dean, 1987; Modified from Moore, 1982)

As a result of relationship between the sediment diameter and the equilibrium depth, the difference between natural beach sand and filled (added) sand diameters creates intersecting ($D_f > D_n$) and non-intersecting ($D_f \leq D_n$) profiles (Figure 2.3).

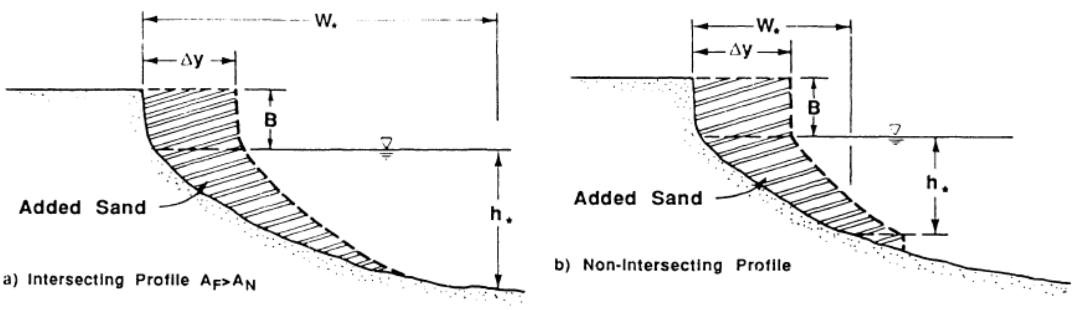

Figure 2.3. Two Generic Types of Nourished Profiles (Dean, 1991)

In Figure 2.3, B is the berm height, Δy is the berm width, h_* is the closure depth, and W_* is the width up to closure depth where sediment transport occurs. Added sand diameter is generally selected coarser than the natural sand diameter in order to intersect bottom profiles before the closure depth and reduce the sand loss.

After a beach reaches its equilibrium profile in still water, increased water level (breaking waves, wave set-up, high tides etc.) may also cause beach erosion and forms a submerged (non-intersecting) profile (Figure 2.4) up to the closure depth (h_* or d_c).

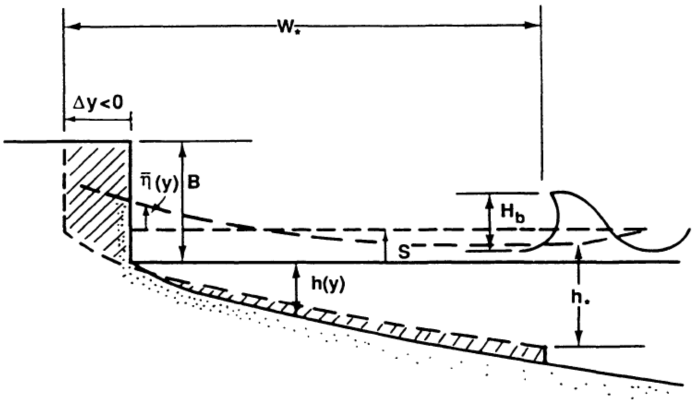

Figure 2.4. Submerged Profile Due to Waves and Increased Water Level (Dean, 1991)

In Figure 2.4, S represents the set-up, η is the surface elevation and H_b is the breaker height. Several studies about closure depth were conducted, yet only the most common two are presented. Birkemeier (1985) modified the relationship between closure depth and Froude number given in Hallermeier (1978), then suggested a formula (Eq. 2.5):

$$d_c = 1.75\,H_s - 57.9\left(\frac{H_s}{gT^2}\right) \qquad \text{Eq. 2.5}$$

Where H_s is the significant wave height. A few years later, CUR (1990) simplified the equation as given in Eq. 2.6:

$$d_c = 1.6\,H_{s,12} \qquad \text{Eq. 2.6}$$

where $H_{s,12}$ represents the significant wave height that occurs 12 hours per year.

If initial nearshore profile is uniform (i.e. bottom slope is constant), equilibrium beach profiles cause recession or progression (advancement) with respect to the original shoreline. Dean (1991) divides equilibrium beach profiles commencing from initially uniform slopes into five different types and illustrates them as Figure 2.5:

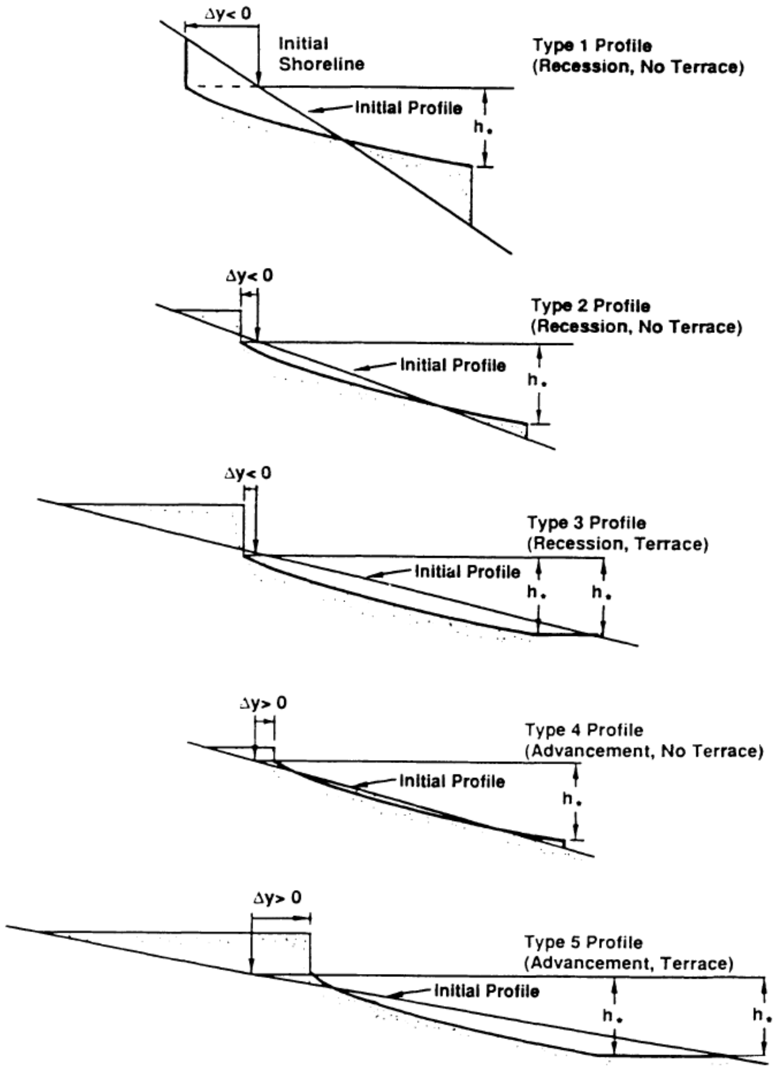

Figure 2.5. Equilibrium Beach Profiles Commencing from Initially Uniform Slopes (Dean, 1991)

As seen in Figure 2.5, "Δy<0" means erosion and "Δy>0" means progression. The eroded sand volume (V_E) equals to deposited sand volume (V_D) for all types of profiles. The illustrated beach profiles are formed seasonally, under the effects of calm (summer) and storm (winter) waves (Sorensen, 2006, see Figure 2.6). Beach profile characteristics are expected to be a function of both wave parameters and sediment properties (Eq. 2.6) as Gourlay parameter (Ω) after the study of Gourlay (1968):

$$\Omega = \frac{H_b}{w_s\, T} \qquad \text{Eq. 2.6}$$

where H_b is the breaking wave height and T is the wave period. Following the model test Wright and Short (1984) carried out, it is stated that when Ω<1, beaches tend to be steep and stable, with foreshore dunes; whereas when Ω>1-2, the eroded sand forms a terrace or sand bar near closure depth (Figure 2.6). Moreover, sand ripples may also be generated nearshore, where wave breaking is frequently observed.

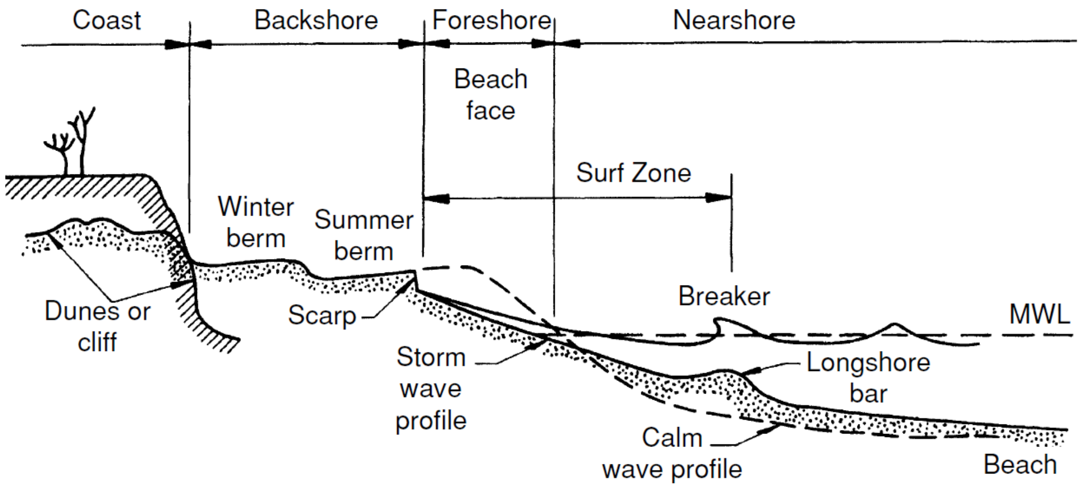

Figure 2.6. Typical Beach Profiles Due to Storm and Calm Waves (Sorensen, 2006)

2.2. Shoreline Protection

When a storm hits the shore, a beach may be eroded as a result of longshore or cross-shore sediment drift. For the shoreline protection, hard (rubble-mound) structures like groins, jetties, detached and submerged breakwaters; and soft (flexible) structures like gravel/pebble beaches, beach nourishment and geotextile sand containers can be used.

If the non-intersecting profile is formed after a beach nourishment application, keeping the filled sand becomes a major problem. Therefore, a toe structure could be designed to create a perched beach by ensuring the filled sand is trapped (Figure 2.7). By doing that, using geotextile sand containers instead of traditional rubble-mound structures gives not only a flexibility in terms of design parameters (e.g. depth), but also a feasible, aesthetic and environment friendly solution (Tayade et al., 2015).

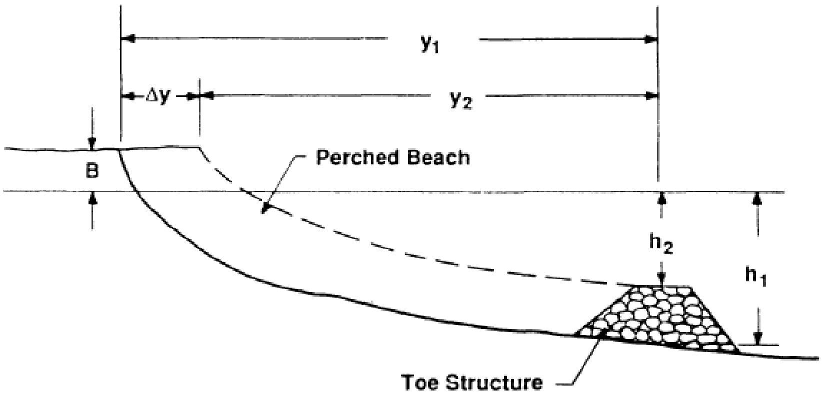

Figure 2.7. Definitional Sketch of a Perched Beach with a Rubble-Mound Toe Structure (Dean, 1991)

2.2.1. Beach Nourishment

Beach nourishment (i.e. beach fill) is placing a sand on a beach to either restore/build a recreational area or offer storm protection by reducing the wave energy nearshore (Dean and Dalrymple, 2001). The placement of sand provided by offshore or onshore sources may be done mechanically (dumping) or hydraulically (pumping). If the filled sand is not lost due to shoreline erosion and necessity of re-nourishment is not emerged around 5-7 years, the project can be considered as successful (Dean, 2002).

Figure 2.8. Placement Methods of Nourished Beaches. Mechanically (Left) and Hydraulically (Right)

According to Nordstrom (2008), the benefits of beach nourishment can be listed as:

- Creating beach or dune where none existed
- Protecting human facilities and burying incompatible human structures
- Protecting dune habitat from wave erosion, providing wider space for full environmental gradients and habitat for rare or endangered species
- Counteracting effects of sea level rise

The main adverse effects of beach nourishment are given as:

- Increasing turbidity and sedimentation
- Changing morphology and sediment characteristics of borrow areas
- Changing morphology, grain size characteristics and dynamic state of beaches

2.2.2. Geotextile Tubes and Geosystems

Since their area of usage in coastal engineering is widening day by day, significant studies and books about geotextile tubes and geosystems are present in the literature.

One of the first studies about geotextile tubes is conducted by Pilarczyk (1995). General information about their advantages, applications and sand filling processes are detailly explained in the study. It is also claimed that geotextile tubes are gaining their ideal shapes when the fullness ratio reaches the 80 percent.

After their popularity rises, geosystems had needed to be worked in detail. Books, articles and design manuals have been written one after another, for instance Lawson (2008) studied three main geotextile containment units (geotextile tubes, geotextile containers and geotextile bags) by analyzing their use in a wide range of hydraulic and environmental applications. The relationships between engineering parameters (see Figure 3.13) and failure mechanisms (Figure 2.9) of geotextile tubes are presented.

Oumeraci and Recio (2009) carried out laboratory experiments about sand containers and discussed their hydraulic stabilities under wave attack. Stability formulae are derived and their area of use in coastal protection is illustrated as Figure 2.10:

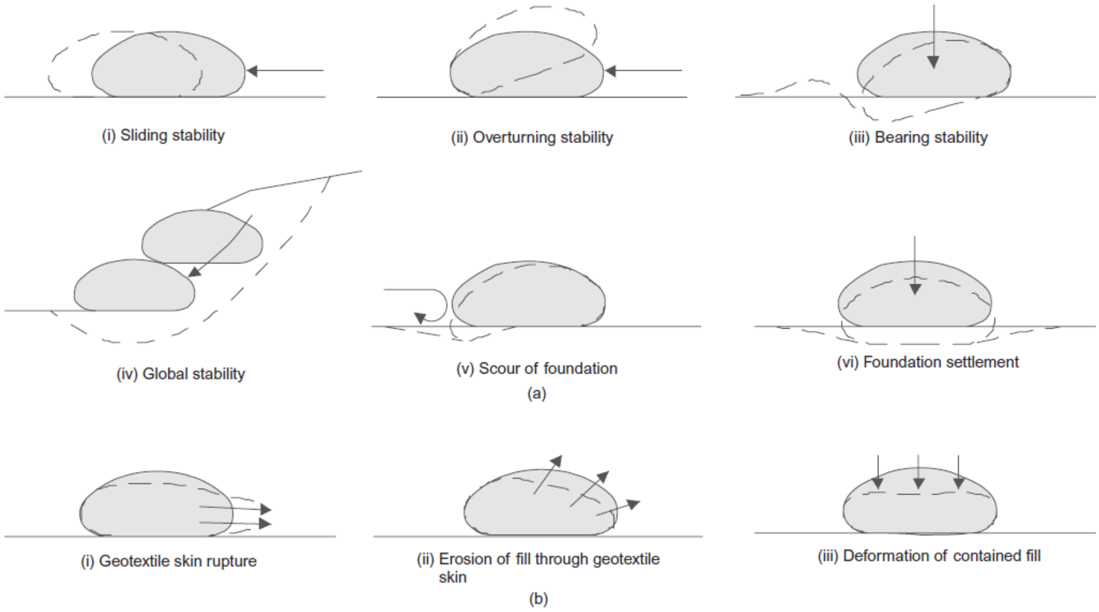

Figure 2.9. External and Internal Failure Mechanisms of Geotextile Tubes (Lawson, 2008)

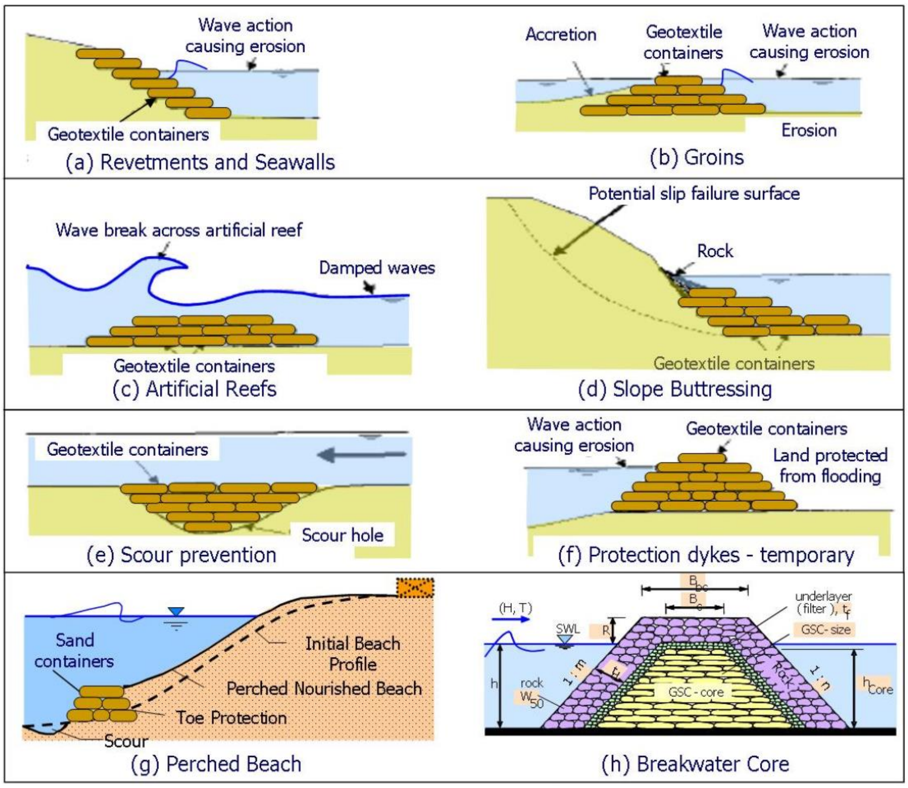

Figure 2.10. Coastal Engineering Applications of Geotextile Sand Bags (Oumeraci and Recio, 2009)

In recent years, books and design manuals are prepared to guide coastal engineers and designers about geosystems. Bezuijen and Vastenburg (2013) prepared a document containing design rules and applications about geosystems and discussed their advantages and performance-based potentials in their study. Then, Koerner (2016) gathered all inter-disciplinary works and prepared the most detailed source of information about geotextiles and their world-wide applications.

2.3. Field Applications and Model Experiments

Over 30 years, substantial studies and model experiments have been conducted about perched beach concept, geosystems and their roles in shore protection. Yet, they have focused mainly on stability performances of geotextile structures rather than morphological changes of shores. Besides the model experiments, several successful field applications were assessed and discussed as case studies.

Sorensen and Beil (1988) conducted a series of tank tests in order to investigate the responses of perched beach profiles under wave attack (Figure 2.11). The results suggested that a perched beach with the sill crest near the still water level can be an effective concept for beach nourishment under appropriate conditions.

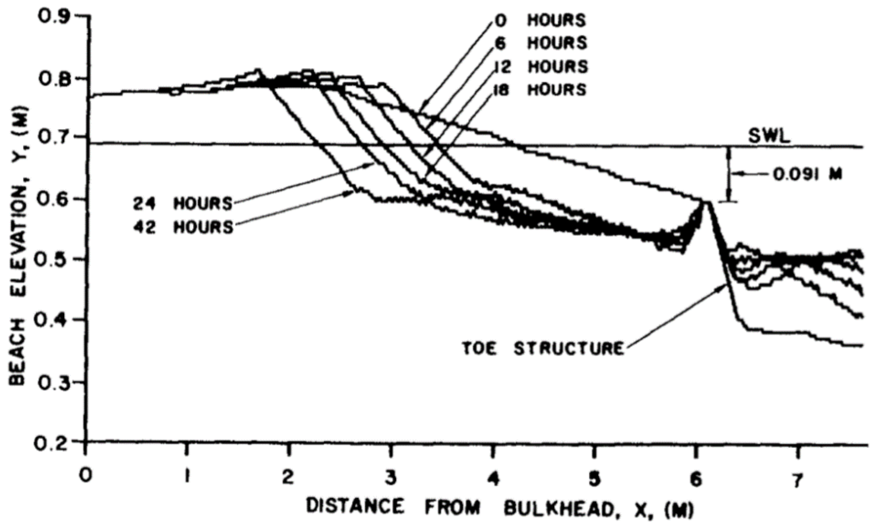

Figure 2.11. Profile Evolution of a Perched Beach under Wave Attack (Sorensen and Beil, 1988)

In the study of González et al. (1999), several laboratory datasets are used to analyze equilibrium condition of a perched beach. The influence of wave breaking over the submerged structure is also discussed (Figure 2.12). It is concluded that advancement is minor for $d/h_c > 0.5$, while considerable advancement is achieved for $d/h_c < 0.1$.

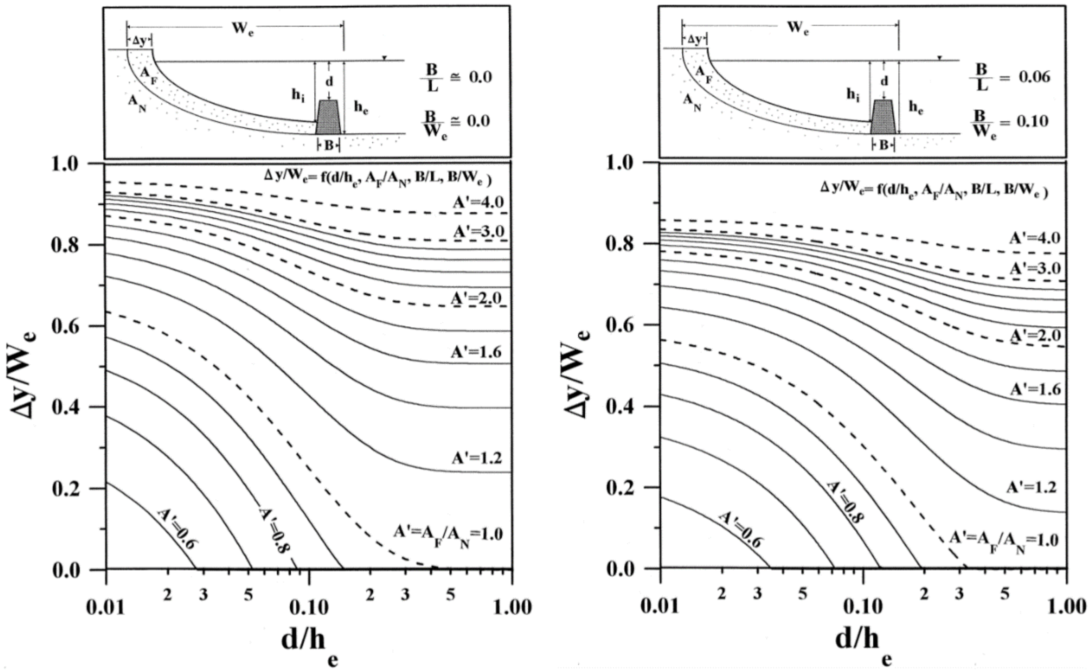

Figure 2.12. Variation of Non-Dimensional Shoreline Advancement (Gonzalez et al., 1999)

Bağcıoğlu (2001) discussed the effects of beach nourishment parameters like sand diameters, profile types (wave height and period), fill volumes and re-nourishment factors. The numerical model, SBEACH (Larson and Kraus, 1989) was applied to Terkos Lake to calculate beach erosion due to storm waves and water level changes. As a result, lack of sand bar formation was found as the main reason of beach erosion.

Hanson et al. (2002) made a detailed analysis of various European beach nourishment projects and practices, explained their objectives. More recently, van Rijn (2014) gathered world-wide experiences and gave examples of successful beach nourishment applications. In addition to sediment transport calculations, certain feasibility assessments were made in the study.

Shin and Oh (2005) conducted a hydraulic model test with different placement methods of geotextile tubes and concluded that stacked geotextile tubes installed with zero-water depth above crest were found to be the most stable and effective for wave absorption. After the study, horizontally double-lined geotextile tubes are used as submerged breakwaters (Figure 2.13) at East Korean Shore (Oh and Shin, 2006).

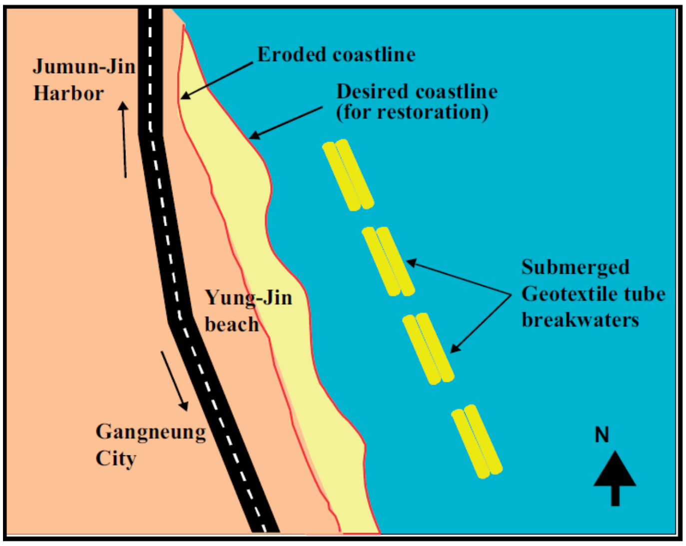

Figure 2.13. Submerged Geotextile Tube Breakwaters in East Korean Sea (Oh and Shin, 2006)

One of the first physical model studies using geotextile tubes in Turkey was carried out by Yalçıner et al. (2006). The tubes were utilized to construct perforated structures and their wave transmission performances are investigated through laboratory tests.

Recio and Oumeraci (2009) carried out physical model experiments in hydraulic laboratory of Leichtweiss-Institute in order to expand the usage of soft structures as shore protection systems. hydraulic stability of sand containers used as a coastal protection structure subject to wave attack. For this purpose, several formulae were proposed about the stability for the slope and crest containers.

Few years after a quasi-3D coastal response model, XBeach (Roelvink et al., 2009) released, Bolle et al. (2011) applied and validated the model for three different field sites (Ostend Beach, Belgium; Elmina Harbour, Ghana and Ada Beach).

For a beach nourishment project at Beidaihe, China, Kuang et al. (2011) studied alternative submerged breakwater designs by using shoreline evolution model named GENESIS (Hanson and Kraus, 1989). As a result, the model might be considered as efficient for simulating a complex nourishment structure system if the model parameters are properly calibrated using either laboratory or field data (Figure 2.14).

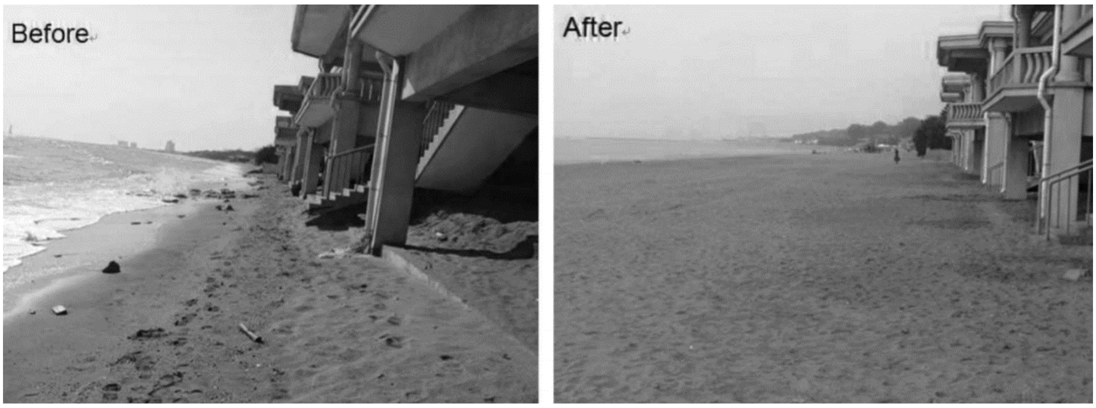

Figure 2.14. Before and After the Beach Nourishment Project (Kuang et al., 2011)

Large-scale physical models of seven configurations are tested in Deltares (van Steeg et al., 2011), in order to identify critical failure mechanisms (Figure 2.15). While all alternatives failed due to sliding, transport of sand within tubes caused no failure. It is also stated that Froude scaling can be applied for small-scale physical models.

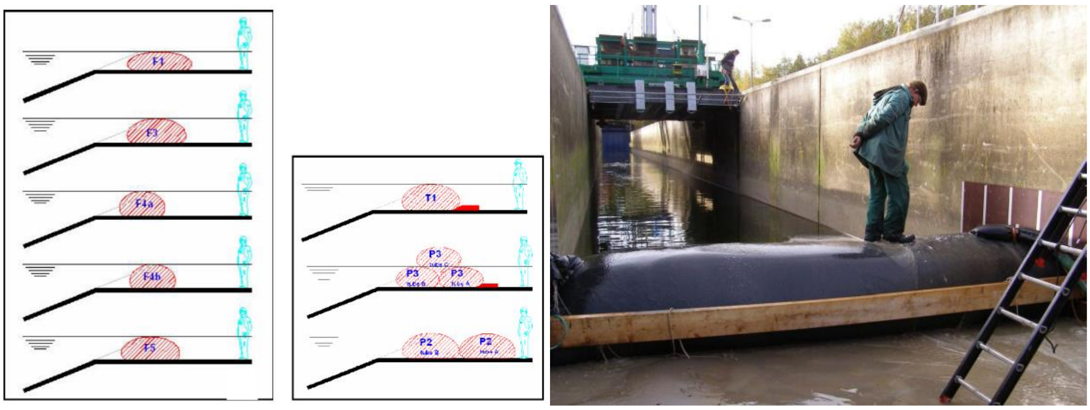

Figure 2.15. Configurations (Left) and Setup (Right) of Large-Scale Tests (van Steeg et al., 2011)

In addition to stability point of view, performance of nearshore geosystems and sea-side scours are also investigated by das Neves (2011) and das Neves et al. (2014). A comparative analysis was studied on efficiency, in other words, maintaining a beach and protecting the shoreline. Based on physical model experiments, the sand-filled geosystems as nearshore submerged structures proved to be efficient in retarding the offshore movement of sediments and in maintaining the shoreline, even if instabilities due to displacements and local scours were observed.

Van Rijn et al. (2011) made numerical simulations of plane sloping beach erosion by irregular wave attack in three wave flumes of different scales. It is concluded that the model performance for the erosive tests are in the range of good to even excellent.

The morphodynamics of a perched nourished beach, located in the southwest coast of Italy, were analyzed by XBeach numerical model (Faraci et al., 2014). By comparing the results with available site surveys, it is stated that; although numerical results well reproduce the slope of the beach profile, they over-predict the erosion in the onshore part of the beach (Figure 2.16).

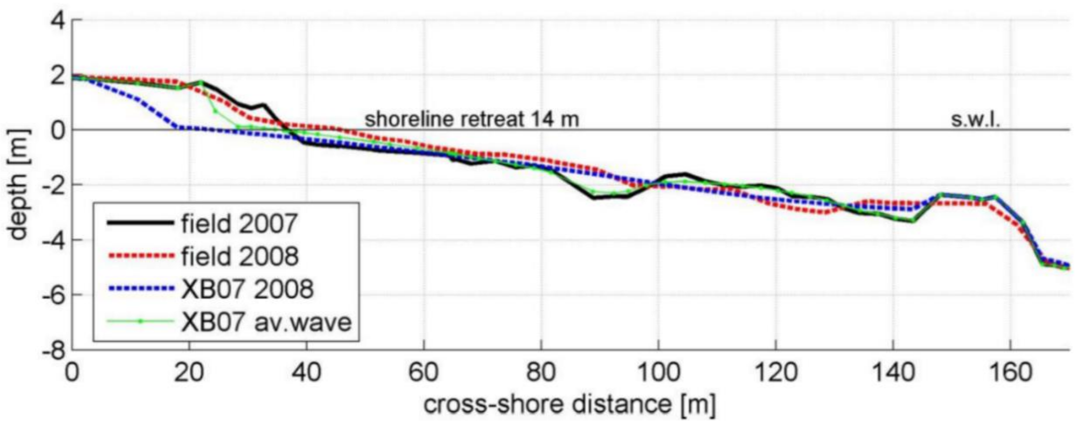

Figure 2.16. Comparison between the Beach Survey and Numerical Results (Faraci et al., 2014)

A scientific support regarding hydrodynamics and sand transport in the coastal zone was prepared by Zimmermann et al. (2015). Evaluating XBeach for long term cross-shore modelling, it is concluded that the slope is realistically reproduced with some calibration, yet XBeach was not able to model coastal erosion due to sea-level rise.

A case study was written by Tayade et al. (2015) about the beach nourishment application in Hamla, India. In this study, importance of geotextile tube location was discussed. It is observed that the performance and life span of geotextile tubes can be enhanced by placing it at MWL or below, as toe structure of beach fill (Figure 2.17).

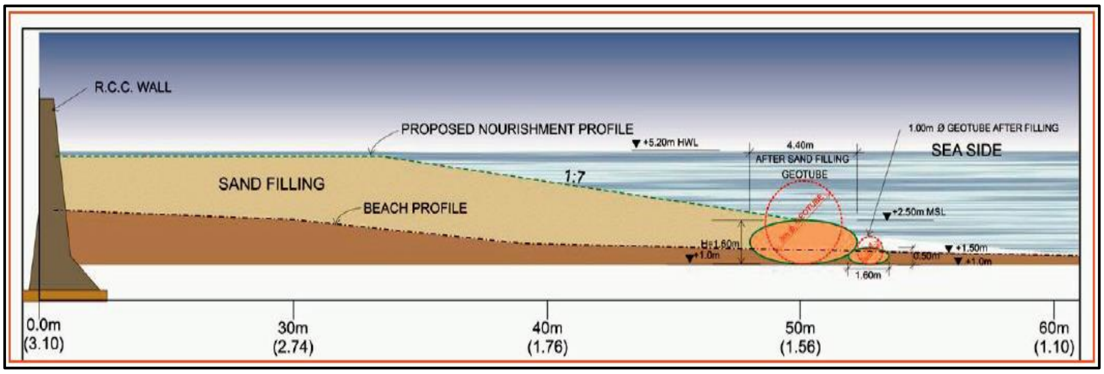

Figure 2.17. Cross-Section of Beach Nourishment Application at Hamla (Tayade et al., 2015)

Giardino et al. (2015) conducted large-scale physical model and numerical beach nourishment model, Delft3D (Figure 2.18). The effects of different nourishment designs, wave conditions, hydrodynamics, sediment transport, grain sorting and morphological development were assessed. It was also implied that the use of modeling is helping in the phase of nourishment design optimization.

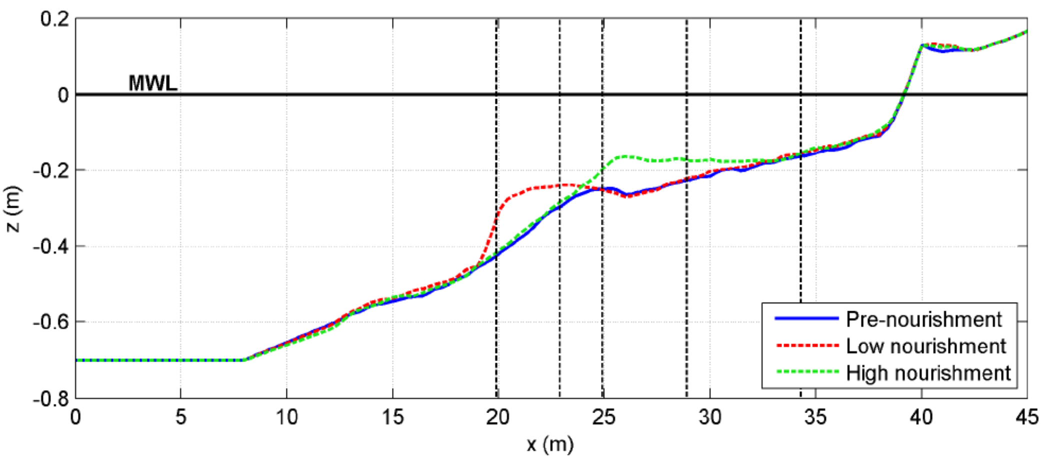

Figure 2.18. Beach Nourishment Design Types (Giardino et al., 2015)

The study performed at Saint-Venant Hydraulic Laboratory (De Carlo et al., 2017) is one of the most recent studies about the subject. The aim was calibrating XBeach model with experimental post-storm profile data to complete numerical simulations of the efficiency of submerged structures. In these experiments, Rouse and Shields parameters were maintained by using low density material, plexi-glass, instead of regular sand, quartz of silicon dioxide (see Chatham, 1972). It was concluded that 2DH experiments and simulations would be necessary to define design criteria and to validate the efficiency of submerged structures (Figure 2.19).

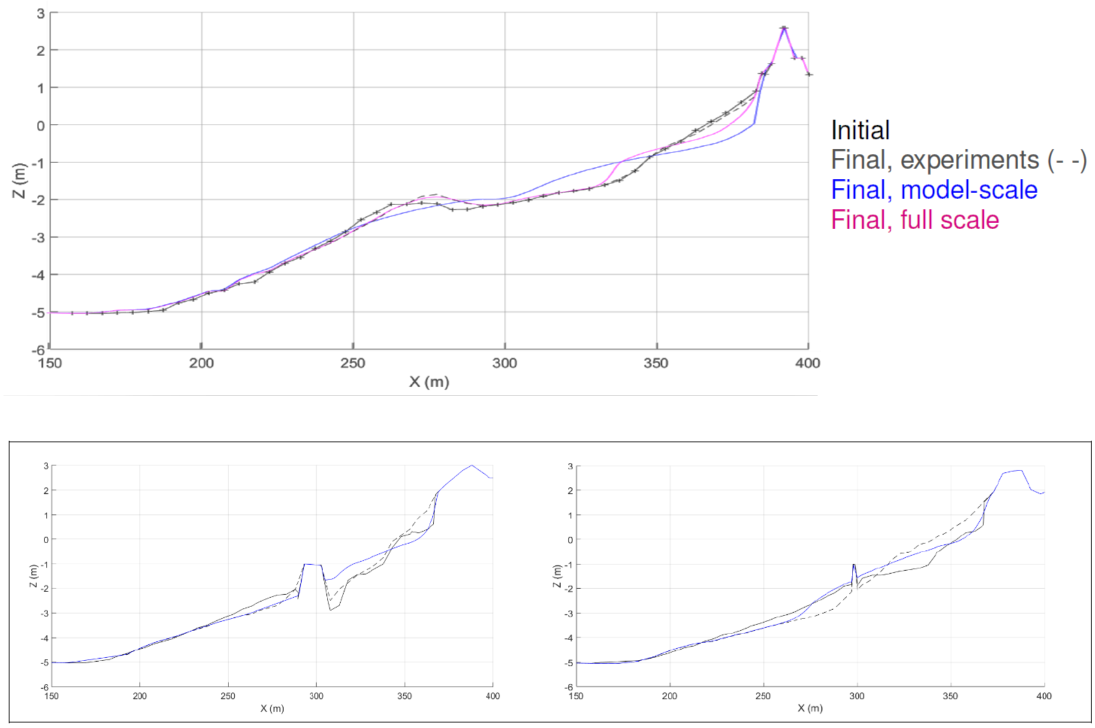

Figure 2.19. Comparison of the Simulated and Measured Beach Profiles (De Carlo et al., 2017)

As a final case study, a beach nourishment and restoration project in Alanya, Turkey is modeled by Baykal et al. (2017) using XBeach. Performances of both offshore breakwaters and geotextile tubes were alternatively investigated in the model study where the subject of this thesis was originated from. Results have shown that the efficiency of the nourishment improves as the grain size of filled sand increases.

CHAPTER 3

PHYSICAL MODEL EXPERIMENTS

3.1. Methodology

In this study, the major problem is set as recession of shoreline and the objective is maintaining the nourished beach profile. Therefore, in order to discuss the performance of soft structures as a toe protection, two-dimensional movable bed physical model experiments are performed changing some of the varying parameters. A conceptual drawing of all varying parameters in physical model experiments is given in Figure 3.1.

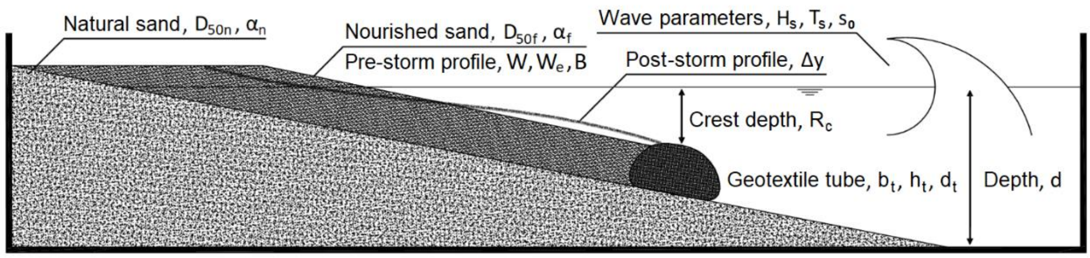

Figure 3.1. Variables of Physical Model Experiments

In Figure 3.1, Wave parameters (H_s, T_s, s) are significant height, significant period and steepness of waves, respectively. Deep-sea wave steepness (s_0) equals to significant wave height divided by deep-sea wavelength ($L_0=1.56T_s^2$). In this study, natural and filled sand median diameters are selected as same ($D_{50n}=D_{50f}=D_{50}$) and berm height (B) was kept constant as the channel depth (d). Therefore, sand berm width (W) and shoreline progression width due to nourishment (W_e) are only depend on the bottom slope (α). Shoreline recession/progression distance (Δy) can be calculated by comparing pre-storm and post-storm profile measurements. Geotextile tube parameters become width (b_t), height (h_t), toe depth (d_t) and crest depth (R_c).

Additionally, densities of water and sand (ρ_s, ρ_w), kinematic viscosity (υ), sediment fall velocity (w_s) and gravitational acceleration (g) are the other governing parameters of the model tests. Considering all basic parameters, dimensional analysis is applied:

$$f_1(H_s,T_s,D_{50},\alpha,W_e,b_t,h_t,d_t,R_c,\rho_w,\rho_s,\upsilon,w_s,g,\Delta y)=0 \qquad \text{Eq. 3.1}$$

Note that, b_t depends on h_t for the experimental setup, since only one geotextile tube is used as a toe structure. This dependency may be changed by using multiple geotextile tubes and configurations, so it is also added to the dimensional analysis.

By applying Buckingham Pi Theorem, nondimensional Pi groups are determined. Choosing ρ_w, g and H_s as repeating parameters, Pi groups have become:

$\Pi_n = \rho_w\ g\ H_s\ \pi_n = 0 \quad \rightarrow \quad [-] = [ML^{-3}]\ [LT^{-2}]\ [L]\ [\pi_n]$

$\Pi_1 = T_s\ (g/H_s)^{1/2}$	$\Pi_2 = D_{50}/H_s$	$\Pi_3 = \alpha$	$\Pi_4 = W_e/H_s$
$\Pi_5 = b_t/H_s$	$\Pi_6 = h_t/H_s$	$\Pi_7 = d_t/H_s$	$\Pi_8 = R_c/H_s$
$\Pi_9 = \rho_s/\rho_w$	$\Pi_{10} = \upsilon\ g^{-1/2}\ H_s^{-3/2}$	$\Pi_{11} = w_s\ (g\ H_s)^{-1/2}$	$\Pi_{12} = \Delta y/H_s$

Then, Eq. 3.1 takes the dimensionless form as:

$$f_2(T_s(g/H_s)^{1/2}, D_{50}/H_s, \alpha, W_e/H_s, b_t/H_s, h_t/H_s, d_t/H_s, R_c/H_s, \rho_s/\rho_w, \upsilon g^{-1/2}H_s^{-3/2}, w_s(gH_s)^{-1/2}, \Delta y/H_s)=0 \qquad \text{Eq 3.2}$$

where $T_s(g/H_s)^{1/2}$ can be written as H_s/gT_s^2 which is known as wave steepness (s).

3.2. Wave Channel and Lab Instrumentation

Physical model experiments are conducted in the wave channel at METU Coastal and Ocean Engineering Laboratory of Civil Engineering Department (Figure 3.2). The channel has 29.0 m length, 6.0 m width, 1.0 m depth and there is 18-m-long and 1.5-m-wide inner channel constructed. At the end of the channel, wave absorbers are placed to minimize the effect of reflected waves. Wave absorbing system was made of plastic wire scrubbers inside of parabola-sloped steel frames.

Figure 3.2. Wave Channel at METU Coastal and Ocean Engineering Laboratory

A piston-type wave generator produced by DHI, which can be generate both regular and irregular waves, is used for physical model experiments (Figure 3.3).

The operational limits of the wave generator are:

Frequency;	0.05 Hz < f < 2.0 Hz	(Wave periods; 0.5 s < T < 20.0 s)
Stroke amplitude;	-290 mm < S_0 < 290 mm	(Wave heights; H < 250 mm)

when first-order wavemaker solution (Hughes, 1993) is applied (Eq. 3.3):

$$\frac{H}{S_0} = \frac{4\, sinh^2\, kd}{sin\, kd + kd} \qquad \text{Eq. 3.3}$$

In Eq. 3.3, k is the wave number which is equal to 2π/L.

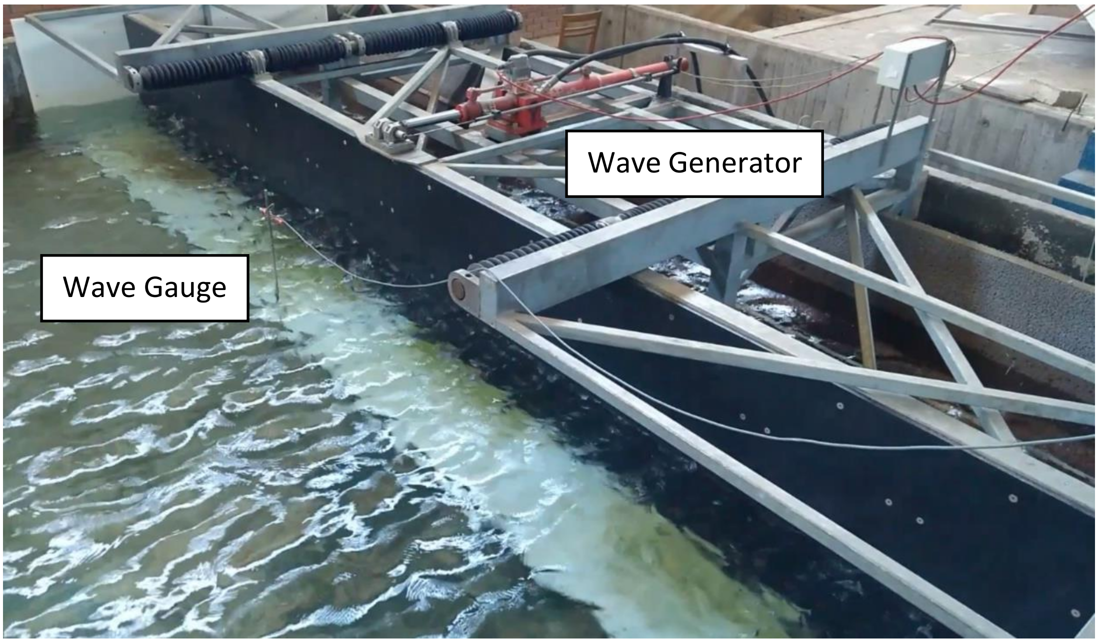

Figure 3.3. Piston-Type Wave Generator and a Wave Gauge

A digital servo controller (Moog SmarTEST ONE) converts digital wave motion data into analog data and transfer them to the piston. While regular wave data can be input using only the controller, time-series of irregular waves need to be input using a computer and a software (e.g. Waveform). In physical model experiments, irregular waves have TMA shallow-water spectra are randomly produced using MATLAB.

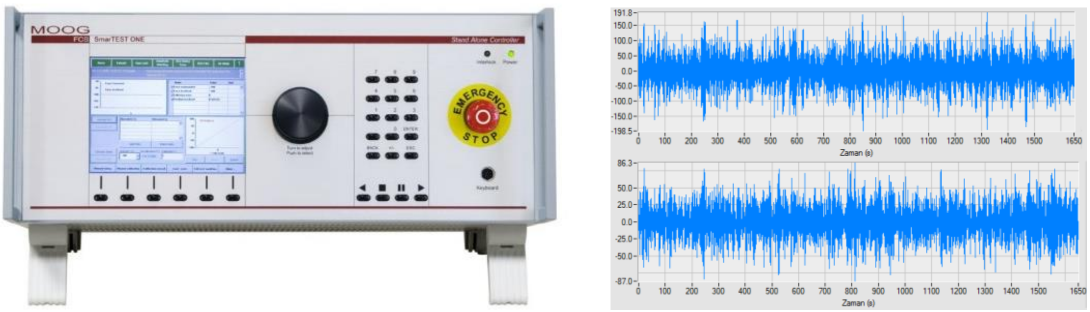

Figure 3.4. Digital Servo Controller (Left) and Time-Series of Irregular Waves (Waveform Interface)

Wave gauges (DHI 202, 600mm) are placed into channel as groups according to Goda and Suzuki (1976) method, in order to make an appropriate wave reflection analysis. For this reason, 3 gauge-couples with 15, 20 and 35 cm distances (first and last gauges are 15 and 20 cm apart from the midst) are placed a wavelength (L) before both geotextile tubes and where bottom slope starts. The voltage data measured by wave gauges can be recorded with a rate of 20 Hz using a software prepared by TDG Scientific Measuring Ltd. After calibrating the recorded data by changing water levels, voltage values can be reconverted into digital wave motion.

3.3. Model Scale

Coastal engineering problems and physical model studies are generally influenced by gravitational and inertial terms, rather than surface tension or viscosity. Therefore, Froude similarity is selected for flume experiments most of the time (Hughes, 1993).

$$Fr = \frac{u}{\sqrt{gd}} \qquad \text{Eq. 3.4}$$

According to Dalrymple and Thompson (1976), using geometric similarity while maintaining Stokes fall velocity (see Eq. 2.3) is the most practical method for sediment transport laboratory tests due to availability of sand. Note that the drag coefficients (C_D) are in Stokes region (i.e. low Reynolds number, Re<1).

$$\lambda_L = \frac{L_m}{L_p} \qquad \text{Eq. 3.5}$$

$$\lambda_T = \sqrt{\lambda_L} \qquad \text{Eq. 3.6}$$

Considering operational limits of the wave generator, depth limits of wave channel (0.3 m < d < 0.7 m), shallow water and breaking conditions of the waves generated, the model length scale was chosen as 1:16. Thus, the time scale has become 1:4. Considering wave parameters and the geometric limits, the depth of still water level of the experimental setup is determined as 0.60 m. Maximum depth has become;

$d = 0.60 * 16 = 9.6\ m$ on prototype scale, which is beyond the depth of closure.

3.4. Experimental Setup

In the context of the physical model experiments, several parameters were going to be compared with each other. These parameters can be grouped under 3 major headlines:

- Storm characteristics;

  Erosive (winter, steep) and accretive (summer, swell) wave profiles.
- Sediment sizes;

  Fine (0.1 mm < D_{50} < 0.25 mm) and coarse (0.5 mm < D_{50} < 1.0 mm) sand
- Geotextile tube dimensions (prototype scale);

  Toe structure (h_t = 2m) and submerged breakwater (h_t = 4m)

For operational reasons, inner channel was also divided into two and 0.60-m-wide channel was prepared for physical model experiments. Section and plan views of wave channel and experimental setup of an example case is given in Figure 3.5.

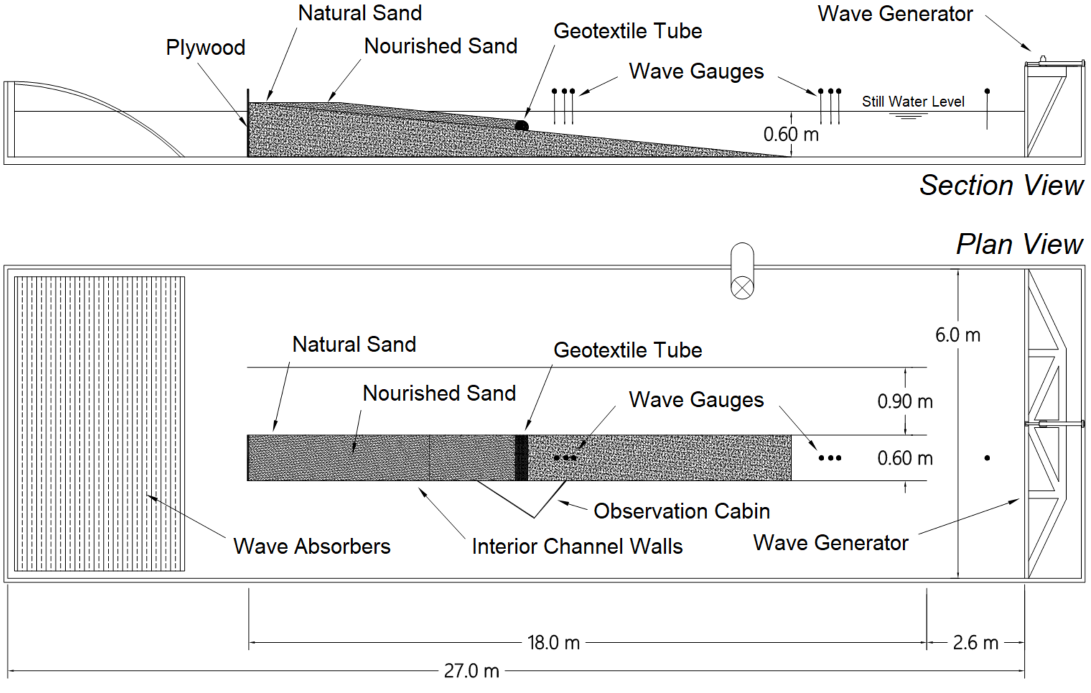

Figure 3.5. Section and Plan Views of Wave Channel with the Experimental Setup

Figure 3.6. Model-Scale Geotextile Tube as Toe Structure of Beach Nourishment

The two of the main experiment materials (beach sand and geotextile tubes) were examined and prepared individually.

3.4.1. Sand Properties

For laboratory experiments, two different type of sand was going to be purchased from Şile, İstanbul where sand quarry of Çeliktaş is located. On related webpage, sieve analysis (Turkish Standards) results of all materials are shared (Table 3.1 and 3.2).

Table 3.1. Sieve Analysis Results of Fine Sands (Turkish Standards)

TS Sieve Size (mm)	AFS 50-55		AFS 60-65		AFS 60-70		AFS 70-80	
	Passing (%)	Retained (%)	Passing (%)	Retained (%)	Passing (%)	Retained (%)	Passing (%)	Retained (%)
0.71	100.0%	0.0%	100.0%	0.0%	100.0%	0.0%	100.0%	0.0%
0.5	98.5%	1.5%	99.5%	0.5%	99.6%	0.4%	99.9%	0.1%
0.355	86.8%	13.2%	96.1%	3.9%	98.4%	1.6%	99.8%	0.2%
0.25	45.1%	54.9%	78.5%	21.5%	84.7%	15.3%	93.1%	6.9%
0.18	6.5%	93.5%	19.5%	80.5%	30.7%	69.3%	55.6%	44.4%
0.125	0.1%	99.9%	4.3%	95.7%	6.9%	93.1%	12.8%	87.2%
0.09	0.0%	100.0%	0.7%	99.3%	1.2%	98.8%	2.3%	97.7%
0.063	0.0%	100.0%	0.2%	99.8%	0.1%	99.9%	0.2%	99.8%
0.001	0.0%	100.0%	0.0%	100.0%	0.0%	100.0%	0.0%	100.0%
D_{50} (mm)	0.266		0.212		0.208		0.155	

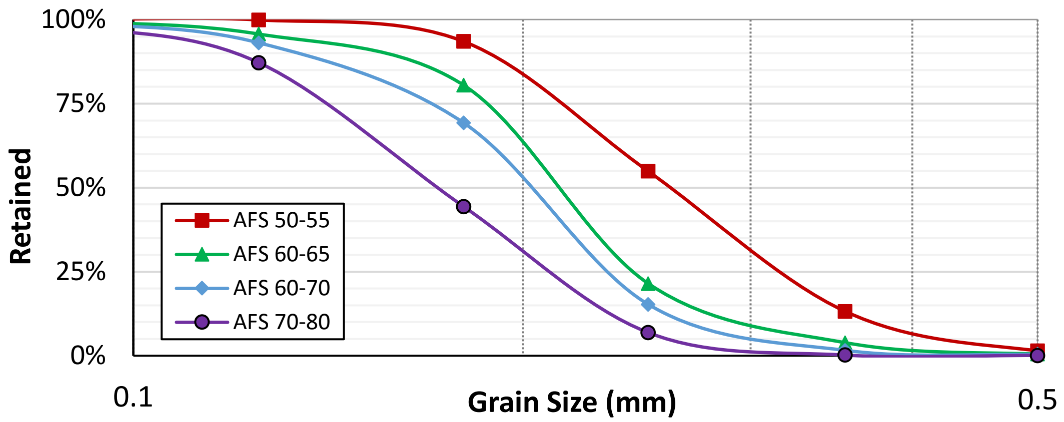

Figure 3.7. Gradation Curves of Fine Sands

Table 3.2. Sieve Analysis Results of Coarse Sands (Turkish Standards)

TS Sieve Size (mm)	AFS 15-20		AFS 20-30		AFS 30-35	
	Passing (%)	**Retained (%)**	**Passing (%)**	**Retained (%)**	**Passing (%)**	**Retained (%)**
2	97.4%	2.6%	99.9%	0.1%	100.0%	0.0%
1.6	90.5%	9.5%	99.3%	0.7%	100.0%	0.0%
1	64.4%	35.6%	90.8%	9.2%	97.2%	2.8%
0.71	33.5%	66.5%	66.8%	33.2%	87.8%	12.2%
0.5	11.5%	88.5%	25.9%	74.1%	59.7%	40.3%
0.355	2.6%	97.4%	4.2%	95.8%	28.3%	71.7%
0.25	0.3%	99.7%	0.5%	99.5%	6.8%	100.0%
0.18	0.0%	100.0%	0.0%	100.0%	0.6%	100.0%
0.001	0.0%	100.0%	0.0%	100.0%	0.0%	100.0%
D_{50} (mm)	0.866		0.614		0.446	

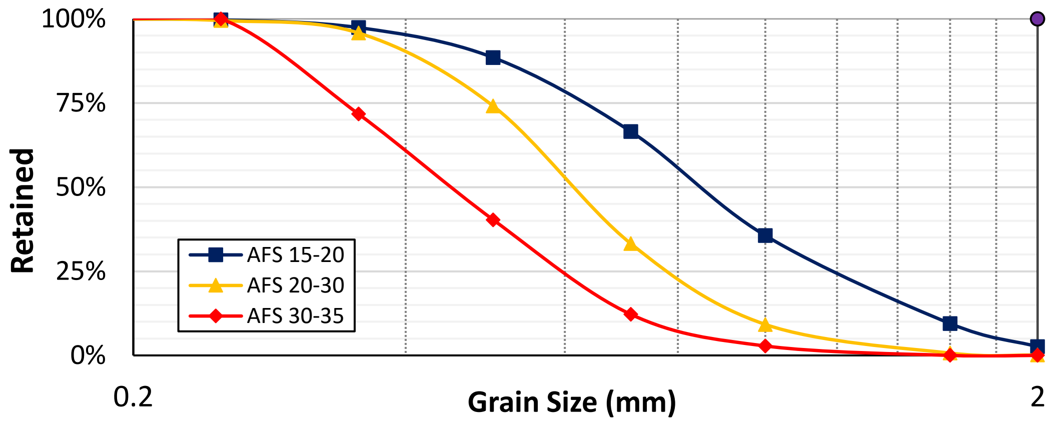

Figure 3.8. Gradation Curves of Coarse Sands

The selection was done, AFS 60-70 as fine sand and AFS 20-30 as coarse sand (see Figure 3.9) are transported to the laboratory.

Figure 3.9. AFS 60-70 as Fine Sand (Left) and AFS 20-30 as Coarse Sand (Right)

Then, before placing them into the wave channel, four samples taken from different bags for fine sand and one mixed sample for coarse sand were passed through several tests like sieve analysis (ASTM), specific gravity and moisture content (Figure 3.10) at METU Construction Materials Laboratory of Civil Engineering Department.

Figure 3.10. Laboratory Tests, Respectively: Sieve Analysis, Moisture Content, Sample Splitting

Sample splitting (See Figure 3.10) was done only for coarse sand since only one sample mix was tested as an average. While results of sieve analyses were given in Table 3.3 and 3.4; gradation curves were drawn as Figure 3.11 and 3.12.

Table 3.3. Sieve Analysis Results of Fine Sand Samples (ASTM)

ASTM Sieve Size (mm)	Sample #1		Sample #2		Sample #3		Sample #4	
	Passing (%)	Retained (%)	Passing (%)	Retained (%)	Passing (%)	Retained (%)	Passing (%)	Retained (%)
0.6	100.0%	0.0%	100.0%	0.0%	100.0%	0.0%	100.0%	0.0%
0.3	86.2%	13.9%	96.8%	3.2%	80.3%	19.8%	93.9%	6.2%
0.15	7.5%	92.5%	11.0%	89.0%	14.2%	85.8%	18.4%	81.6%
0.075	0.3%	99.7%	0.3%	99.7%	0.4%	99.7%	0.4%	99.6%
0.001	0.0%	100.0%	0.0%	100.0%	0.0%	100.0%	0.0%	100.0%
D_{50} (mm)	0.196		0.198		0.207		0.203	

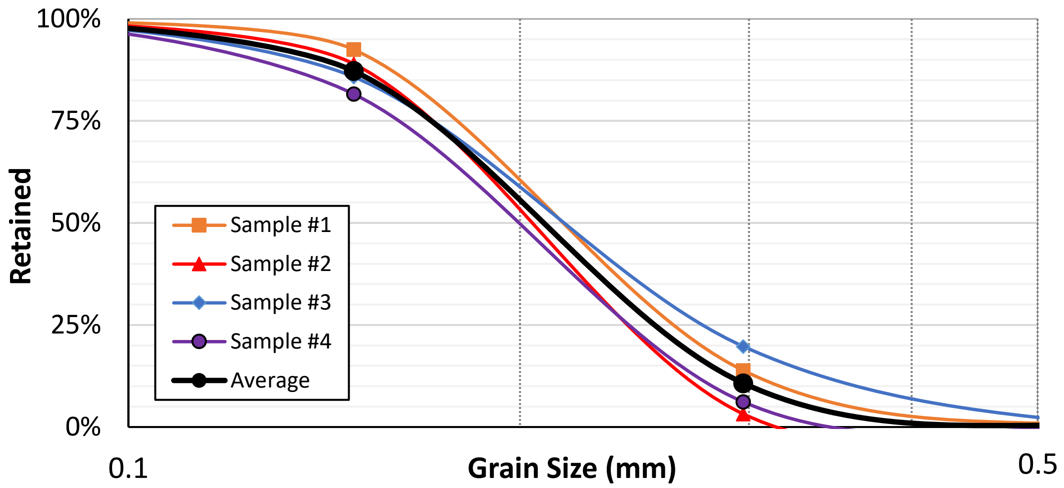

Figure 3.11. Gradation Curves of Fine Sand Samples

Table 3.4. Sieve Analysis Results of Coarse Sand Sample (ASTM)

ASTM Sieve Size (mm)	Mixed Sample	
	Passing (%)	Retained (%)
2.4	100.0%	0.0%
1.2	95.2%	4.8%
0.6	41.9%	58.1%
0.3	1.3%	98.7%
0.15	0.1%	99.9%
0.075	0.0%	100.0%
D_{50} (mm)	0.692	

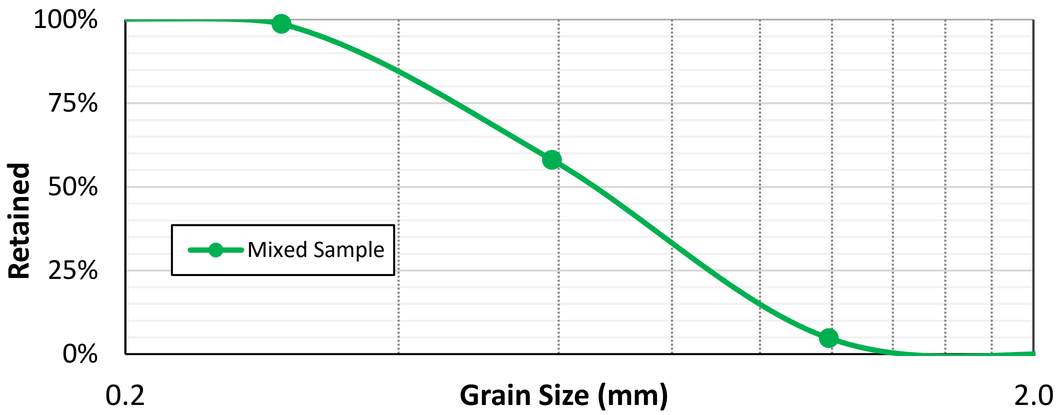

Figure 3.12. Gradation Curve of Coarse Sand Sample

Besides the grain diameters, other physical properties of sand samples are summarized in Table 3.5.

Table 3.5. Physical Properties of Sand Samples

Physical Property	**Fine Sand**	**Coarse Sand**
Median grain size, D_{50} (mm)	0.20	0.65
Specific gravity, SG (-)	2.66	2.65
Unit weight of loose sand, γ_{sat} (kN/m^3)	13.45	N/A
Unit weight of dry sand, γ_d (kN/m^3)	14.90	N/A
Absorption capacity (%)	0.73	0.47

3.4.2. Geotextile Tubes

The engineering parameter relationships (Lawson, 2008) were given in Figure 3.13.

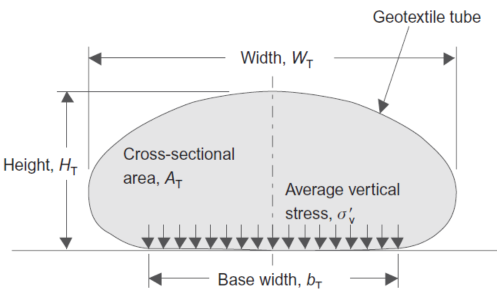

Engineering parameter	In terms of theoretical diameter, D_T
Maximum filled height, H_T	$H_T \approx 0.55\ D_T$
Filled width, W_T	$W_T \approx 1.5\ D_T$
Base contact width, b_T	$b_T \approx D_T$
Cross-sectional area, A_T	$A_T \approx 0.6\ D_T^2$
Average vertical stress at base, σ'_v	$\sigma'_v \approx 0.7\gamma D_T$

Note: γ = bulk density of the geotextile tube fill.

Figure 3.13. Definitional Sketch of Geotextile Tube Engineering Parameters (Lawson, 2008)

Necessary geotextile materials were provided by TenCate Geosynthetics officials. The tube that used in experiments (Figure 3.15) is prepared by a tailor. Geotextile fabrics (Figure 3.14) were sewed to each other for keeping the filled sediment inside the tube. No damage and no movement of geotextile tubes were observed during the tests.

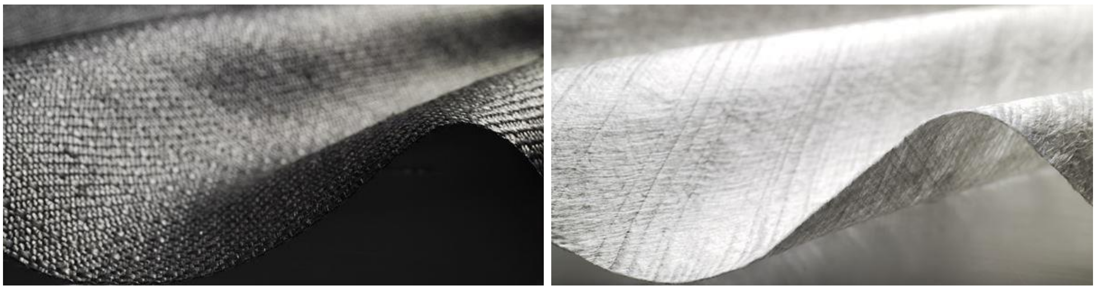

Figure 3.14. TenCate's Geotextile Materials: Geolon PP15 (Left) and Polyfelt TS10 (Right)

Figure 3.15. Side (Left) and Top (Right) Views of a Lab-Scale Geotextile Tube

3.5. Profile Measurement

Both before and after the storm, cross-shore bottom profiles are measured at every 3 to 6 cm (0.5~1.0 m in prototype scale) by sliding a laser meter (Bosch GLM 100 C, Figure 3.16) on a straight line. These measurement data can be stored in a mobile application called Measuring Master (Bosch) and obtained as table format at any time. 3 measurement lines (15 cm in between, avoiding any boundary effects) are used and their averages are drawn to see all profile changes and recession/progression distances.

Figure 3.16. Laser Meter (Bosch GLM 100 C) and Measuring Application

3.6. Data Post-Processing

In the physical model experiments, the calibrated digital wave data are analyzed using a MATLAB routine, which is consist of correction of mean water level, calculation of spectral parameters (e.g. skewness), determination of individual wave heights and periods using zero down-crossing method (IAHR/PIANC, 1986), calculation of significant and root-mean-square wave heights, spectrum analysis (Goda, 2000) and reflection analysis (Goda and Suzuki, 1976).

CHAPTER 4

RESULTS AND DISCUSSION

Effects of varying parameters in beach nourishment applications were investigated through physical model experiments. The tests were divided into 5 stages by changing one variable at a time. In total, effects of 6 parameters (H_s, s_0, D_{50}, α_f, R_c and d_t) were compared using different setups and combinations (Table 4.1).

Table 4.1. Varying Parameters of Physical Model Experiments (Prototype Scale)

Exp.Stage	**Variables**	**D_{50} (mm)**	**H_s (m)**	**s_0**	**d_t (m)**	**R_c (m)**	**α_f**	**W_e (m)**
Stage 1	Wave Conditions (H_s, T_s, s_0)	0.4	3.0	0.04	-	-	-	-
		0.4	2.0	0.04	-	-	-	-
		0.4	1.0	0.04	-	-	-	-
		0.4	1.0	0.03	-	-	-	-
		0.4	1.0	0.02	-	-	-	-
		0.4	1.0	0.01	-	-	-	-
Stage 2	Grain Size (D_{50})	1.3	3.0	0.04	-	-	-	-
		1.3	2.0	0.04	-	-	-	-
		1.3	1.0	0.04	-	-	-	-
		1.3	1.0	0.03	-	-	-	-
		1.3	1.0	0.02	-	-	-	-
		1.3	1.0	0.01	-	-	-	-
Stage 3	Fill Slope (α_f)	1.3	3.0	0.04	4	2	1:15	19.2
		1.3	3.0	0.04	4	2	1:10	28.8
		1.3	3.0	0.04	4	2	1:5	38.4
		1.3	1.0	0.01	4	2	1:15	19.2
		1.3	1.0	0.01	4	2	1:10	28.8
		1.3	1.0	0.01	4	2	1:5	38.4
Stage 4	Toe/Crest Depth (d_t, R_c)	1.3	3.0	0.04	6	4	1:10	28.8
		1.3	1.0	0.01	6	4	1:10	28.8
		1.3	3.0	0.04	6	2	1:10	28.8
		1.3	1.0	0.01	6	2	1:10	28.8
Stage 5	Presence of Tube	1.3	3.0	0.04	-	-	1:10	28.8
		1.3	1.0	0.01	-	-	1:10	28.8

4.1. Wave Calibration

Before taking any profile measurements, the beach with a constant slope (m=1:15) and consist of fine sand was set up into the channel in order to imitate wave reflection from the beach; then wave calibration experiments were held. All measurements were taken at deep-sea (maximum wavelength before the beach slope starts), where the distance from wave generator is also sufficiently long and cause no distortion. Data post-processing was done as explained in Chapter 3.6; accordingly, 6 irregular wave sets (i-vi) with different wave heights, periods and steepnesses are selected to use in next stages of the experiments (Figure 4.1 and 4.2). The selected irregular wave sets for both laboratory and prototype scales are given in Table 4.2 and Table 4.3.

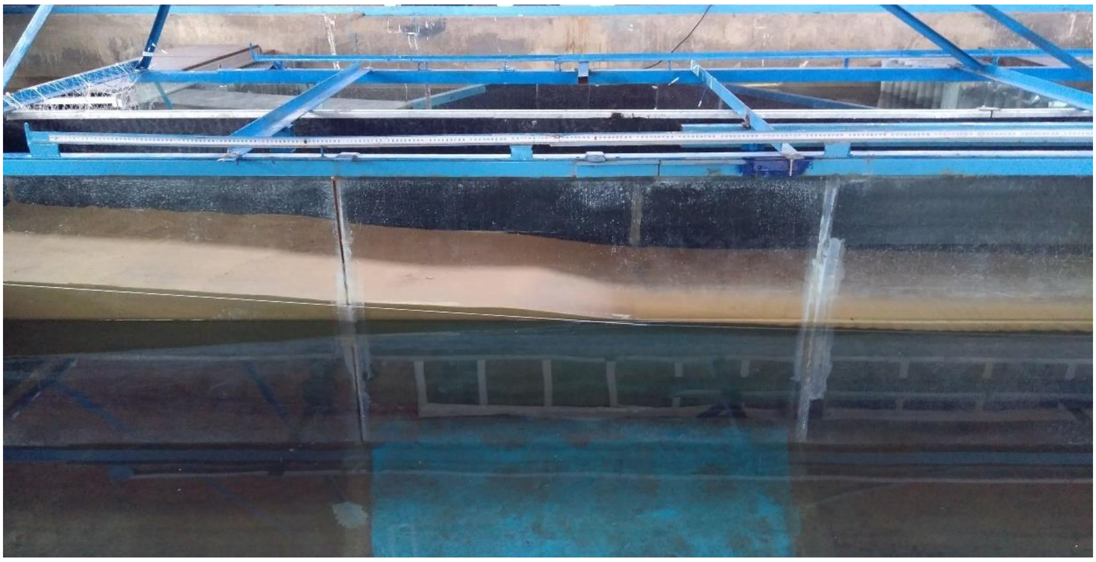

Figure 4.1. Wave Calibration Experiments

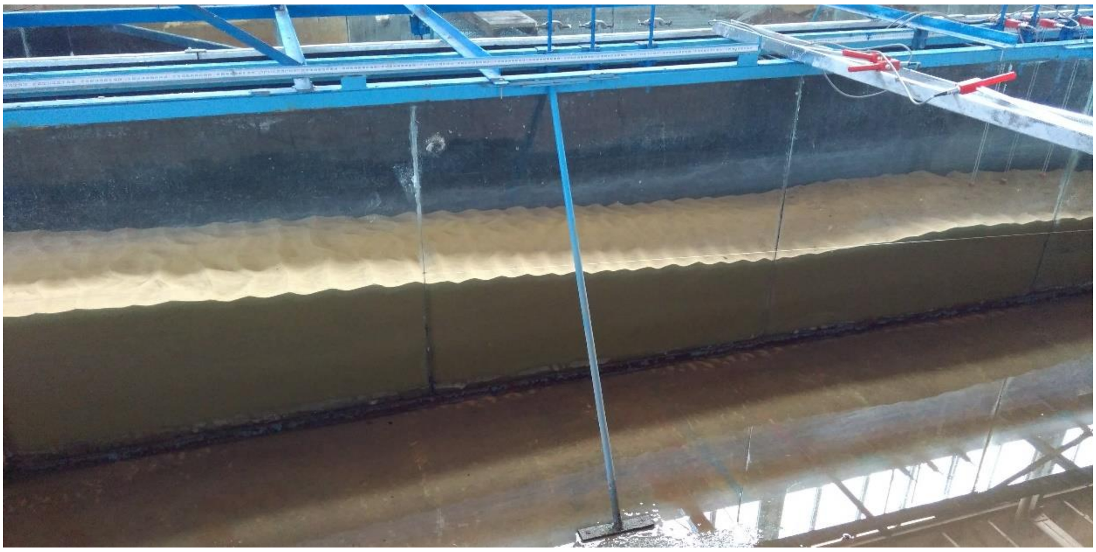

Figure 4.2. Post-storm Profile of Wave Calibration Experiments

Table 4.2. Wave Calibration Results (Model Scale)

Wave	**H_s (m)**	**H_{m0} (m)**	**H_{max} (m)**	**H_{max}/H_s**	**T_s (s)**	**T_m (s)**	**T_p (s)**	**$T_{m,-1-0}$ (s)**	**K_r**
i	0.188	0.184	0.266	1.42	1.73	1.52	1.85	1.66	0.11
ii	0.125	0.126	0.221	1.77	1.41	1.31	1.47	1.36	0.12
iii	0.062	0.063	0.120	1.93	1.00	0.96	1.03	0.98	0.09
iv	0.063	0.064	0.123	1.97	1.16	1.10	1.23	1.14	0.08
v	0.063	0.064	0.115	1.83	1.41	1.28	1.52	1.38	0.07
vi	0.062	0.064	0.101	1.62	2.00	1.67	2.57	2.08	0.10

Table 4.3. Wave Calibration Results (Prototype Scale)

Wave	**H_s (m)**	**H_{m0} (m)**	**H_{max} (m)**	**L_0 (m)**	**T_s (s)**	**T_m (s)**	**T_p (s)**	**$T_{m,-1-0}$ (s)**	**s_0**
i	3.00	2.95	4.26	75.0	6.93	6.07	7.40	6.65	0.04
ii	2.00	2.02	3.54	50.0	5.66	5.22	5.90	5.45	0.04
iii	1.00	1.01	1.93	25.0	4.00	3.86	4.13	3.93	0.04
iv	1.00	1.03	1.97	33.3	4.62	4.39	4.92	4.57	0.03
v	1.00	1.02	1.84	50.0	5.66	5.14	6.07	5.51	0.02
vi	1.00	1.02	1.62	100.0	8.00	6.68	10.26	8.32	0.01

4.2. Wave Conditions

In the first stage of experiments, it is aimed to determine the storm wave characteristics to be used for the next stages. The storm waves that may cause erosion or accretion are modeled and the cross-shore bottom profile changes after the storms are measured and examined. Fine-grained sand with an average grain size of 0.2 mm (on model scale) is placed into the channel with a constant bed slope of 1:15. First, the wave steepness of the storm and the number of waves reaching the shore (N) are kept constant, only the significant wave heights (H_s) and accordingly wave periods (T) are changed in order to see the effects of wave heights on natural beaches. For the second part of Stage-1, significant wave height is kept constant, wave periods and accordingly wave steepnesses are altered to make comparison between different wave parameters. After the first stage of experiments completed, two wave sets are selected as erosive (winter) and accretive (summer) wave profiles for the next stages of physical model experiments. The test parameters used were given in Table 4.4 and Table 4.5.

Table 4.4. Stage-1 Experiment Parameters (Prototype Scale)

Wave	**α_n**	**D_{50} (mm)**	**H_s (m)**	**s_0**
i	1:15	0.40	3.0	0.04
ii	1:15	0.40	2.0	0.04
iii	1:15	0.40	1.0	0.04
iv	1:15	0.40	1.0	0.03
v	1:15	0.40	1.0	0.02
vi	1:15	0.40	1.0	0.01

Table 4.5. Stage-1 Experiment Parameters (Model Scale)

Wave	**α_n**	**D_{50} (mm)**	**H_s (cm)**	**s_0**
i	1:15	0.20	18.75	0.04
ii	1:15	0.20	12.50	0.04
iii	1:15	0.20	6.25	0.04
iv	1:15	0.20	6.25	0.03
v	1:15	0.20	6.25	0.02
vi	1:15	0.20	6.25	0.01

4.2.1. Wave Height

Pre-storm and post-storm cross-shore bottom profiles of waves with different significant wave heights having same wave steepnesses, s_0=0.04 (Figure 4.3 to 4.5) are drawn on the same graph and given in Figure 4.6.

Figure 4.3. Post-Storm Profile of Wave-(i) (Hs=3m and s=0.04 on Prototype Scale)

Figure 4.4. Post-Storm Profile of Wave-(ii) (Hs=2m and s=0.04 on Prototype Scale)

Figure 4.5. Post-Storm Profile of Wave-(iii) (Hs=1m and s=0.04 on Prototype Scale)

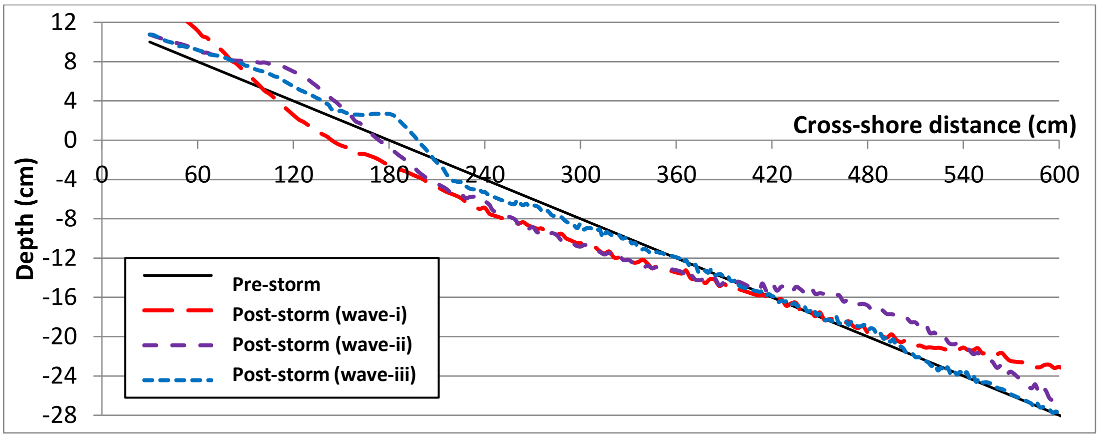

Figure 4.6. Effects of Wave Heights (Fine Sand, D_{50} = 0.2 mm on Model Scale)

Table 4.6. Recession(-)/Progression(+) Distances (Prototype Scale) – Waves i-ii-iii

Wave	D_{50} (mm)	w_s (m/s)	H_s (m)	s_0	α_n	Δy (m)
i	0.4	0.06	3.0	0.04	1:15	-7.8
ii	0.4	0.06	2.0	0.04	1:15	-1.0
iii	0.4	0.06	1.0	0.04	1:15	0.8

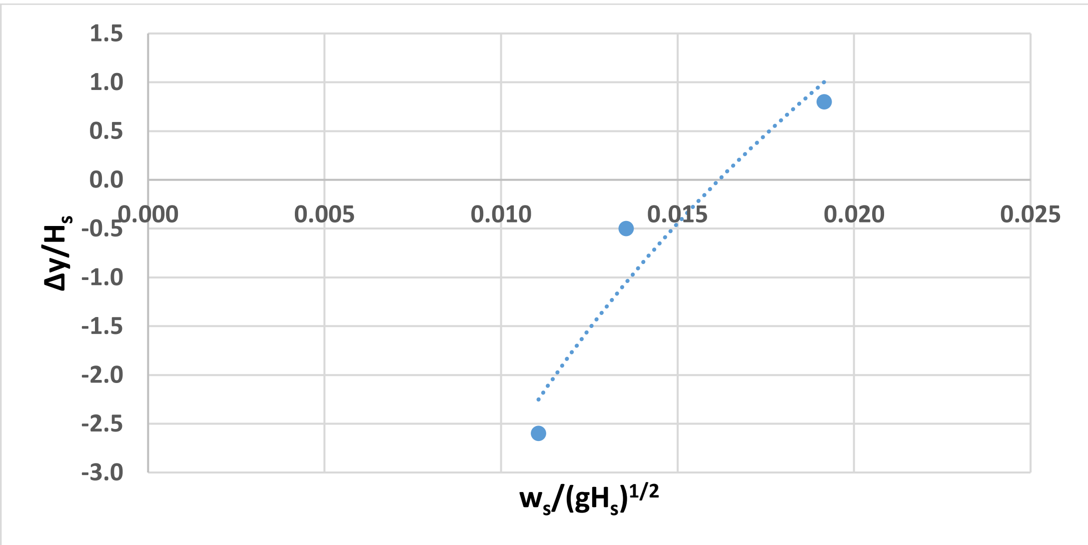

Figure 4.7. Effects of Significant Wave Height (H_s) – s_0=0.04, w_s=0.06 m/s

By looking at Figure 4.6 and Figure 4.7, the changes in the bottom profile of storm waves with the same wave steepnesses and different significant wave heights are examined and the erosion/accretion distances measured at the shoreline, it can be clearly said that the higher significant wave height increased the sediment movement nearshore and caused the recession of the shoreline. Considering the amount of erosion and recession distance of the shore, wave-(i) with a significant wave height of 3 m (s=0.04) was determined as eroding (winter) wave.

Note that, number of waves are constant (10000) for all storms based on the observations and measurements of calibration experiments. In these experiments, it is seen that the bottom profiles reach their equilibrium after approximately 10000 waves.

4.2.2. Wave Steepness

Pre-storm and post-storm cross-shore bottom profiles of waves with different wave steepnesses having same wave heights, H_s = 1.0 m in prototype scale (Figure 4.8 to 4.10) are drawn on the same graph and given in Figure 4.11.

Figure 4.8. Post-Storm Profile of Wave-(iv) (Hs=1m and s=0.03 on Prototype Scale)

Figure 4.9. Post-Storm Profile of Wave-(v) (Hs=1m and s=0.02 on Prototype Scale)

Figure 4.10. Post-Storm Profile of Wave-(vi) (Hs=1m and s=0.01 on Prototype Scale)

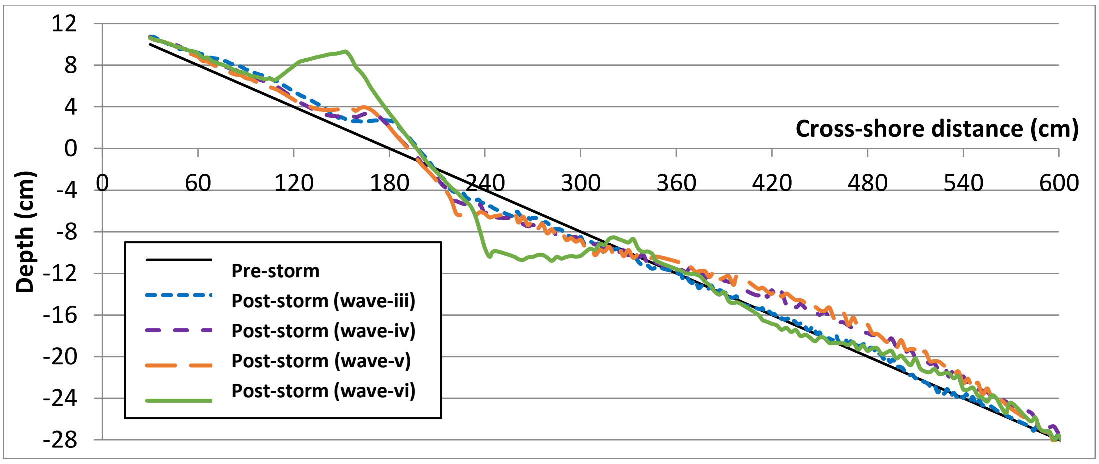

Figure 4.11. Effects of Wave Steepnesses (Fine Sand, D_{50}=0.2 mm on model scale)

Table 4.7. Recession(-)/Progression(+) Distances (Prototype Scale) – Waves iii to vi

Wave	D_{50} (mm)	w_s (m/s)	H_s (m)	s_0	α_n	Δy (m)
iii	0.4	0.06	1.0	0.04	1:15	0.8
iv	0.4	0.06	1.0	0.03	1:15	1.6
v	0.4	0.06	1.0	0.02	1:15	2.2
vi	0.4	0.06	1.0	0.01	1:15	2.8

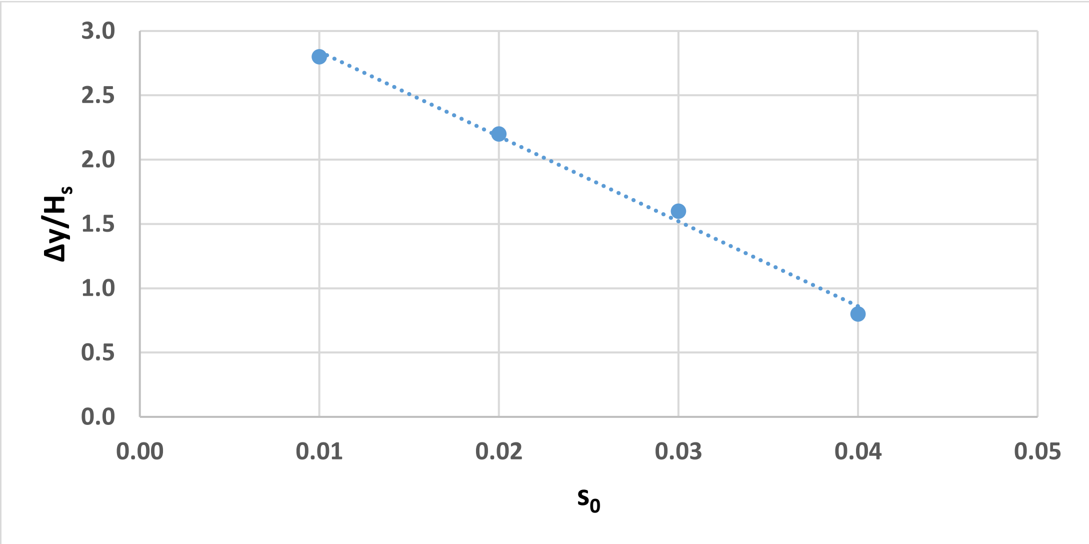

Figure 4.12. Effects of Deep-Sea Wave Steepness (s_0) – H_s=1 m

According to both Figure 4.11 and Figure 4.12, when significant wave height of the accretive waves is constant, but the decrease in wave steepness affected the recession distances slightly, however increased the amount of sand accumulated on the shore at a high rate. Considering the nearshore sand movements and the accretion distance along the shore line, wave-(vi) with 0.01 wave steepness (H_s=1m) was determined as accretive (summer) wave (Figure 4.13).

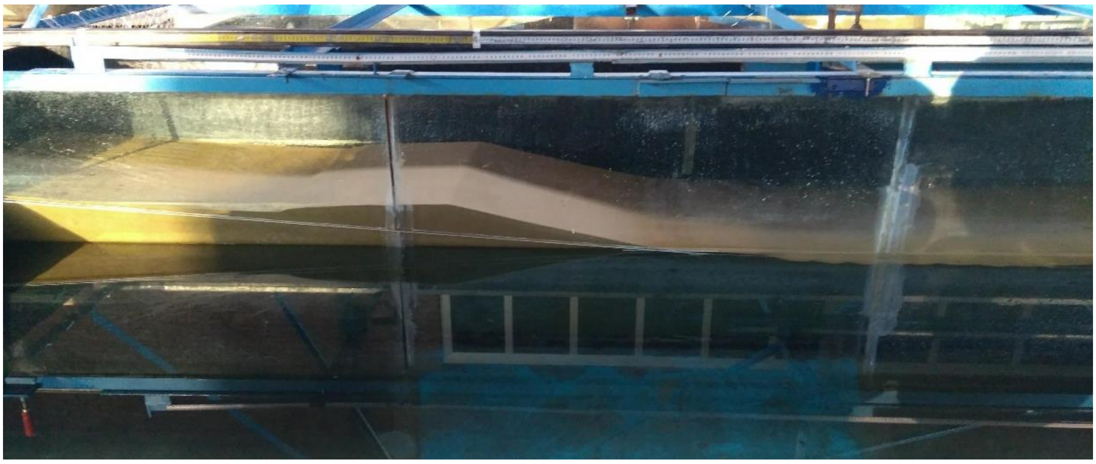

Figure 4.13. Post-Storm Profile of Accretive Waves (Hs=1m and s=0.01 on prototype scale)

4.3. Grain Size

In the second stage of the experiments, average grain size of sand is altered. First stage experiments were repeated with coarse sand having an average grain diameter of 0.65 mm on model scale. Starting from the Stage-2, the number of waves in all storms applied to the model is fixed to 6000 by reason of equilibrium profiles (Figure 4.14). The changing bottom profiles under the influence of different storm waves are presented in Figure 4.15 and Figure 4.16 comparatively. While first and second stage experiments aimed not only to determine the erosion/accretion characteristics of storm waves with different parameters, but also compare fine and coarse sand post-storm bottom profiles. The used parameters were given in Table 4.8 on model scale.

Table 4.8. Stage-2 Experiment Parameters (Model Scale)

Wave	α_n	D_{50} (mm)	H_s (cm)	s_0
i	1:15	0.65	18.75	0.04
ii	1:15	0.65	12.50	0.04
iii	1:15	0.65	6.25	0.04
iv	1:15	0.65	6.25	0.03
v	1:15	0.65	6.25	0.02
vi	1:15	0.65	6.25	0.01

Figure 4.14. Post-Storm Profile of Erosive Waves (Hs=3m and s=0.04 on Prototype Scale)

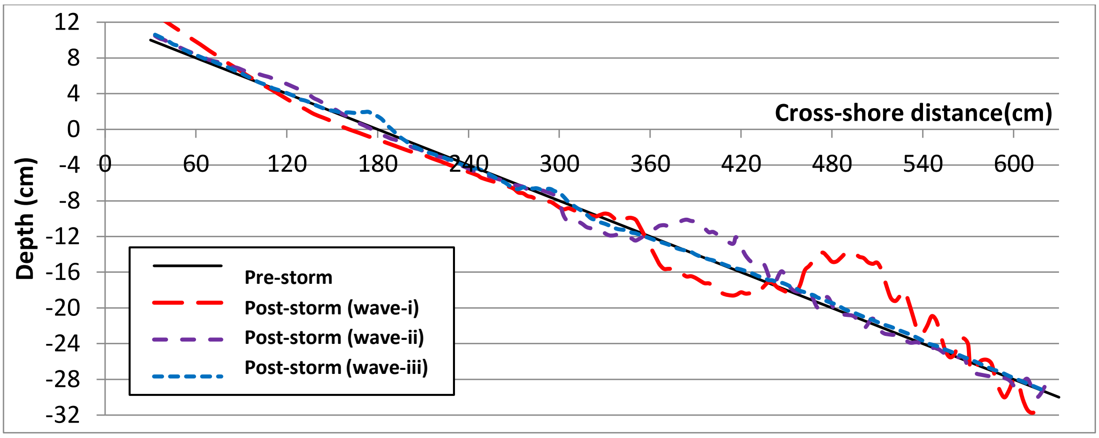

Figure 4.15. Effects of Wave Heights (Coarse Sand, D_{50}=0.65 mm on Model Scale)

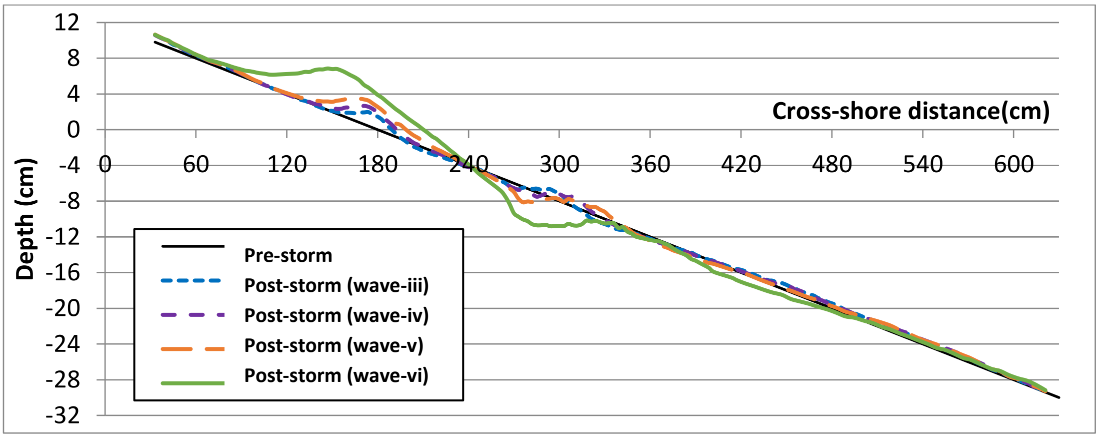

Figure 4.16. Effects of Wave Steepnesses (Coarse Sand, D_{50}=0.65 mm on Model Scale)

When the changes caused by storm waves having the same wave steepness and different significant wave heights in the coarse sand bottom profile are examined, it is seen that the erosion/accretion distances on the shoreline and the sediment movement nearshore are reduced. While the scours and ripples formed by the waves at breaking depths become more apparent and steeper, it is measured that the amount of eroded sand increases with the increase in the significant wave height, as well as with the experiments performed with fine sand. The changes in the coarse sand bottom profile of the accretive waves having the same significant wave height and different wave steepnesses are examined and it is seen that second stage gives parallel results with the first stage experiments. While a large part of the sand movement takes place nearshore, the size of the ripples due to reduced sand movement in the deeper regions has decreased. Therefore, Stage-2 experiments both validate the Stage-1 experiments and give comparative results between two grain sizes (Figure 4.17 and Figure 4.18).

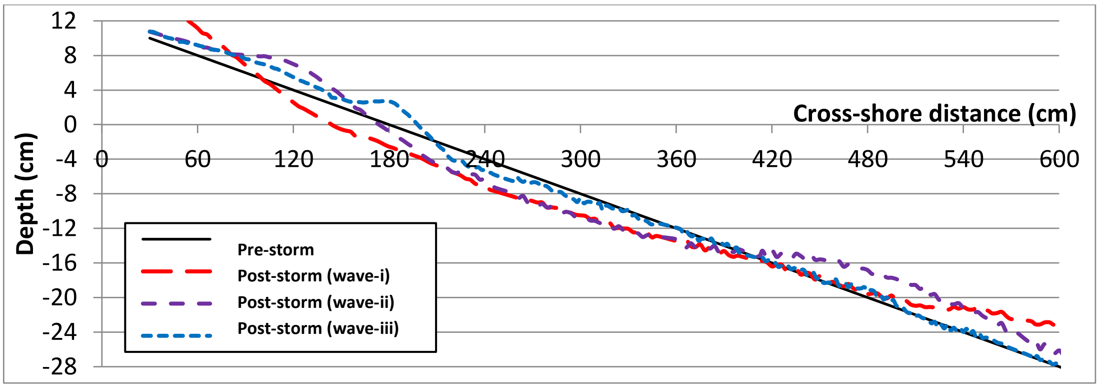

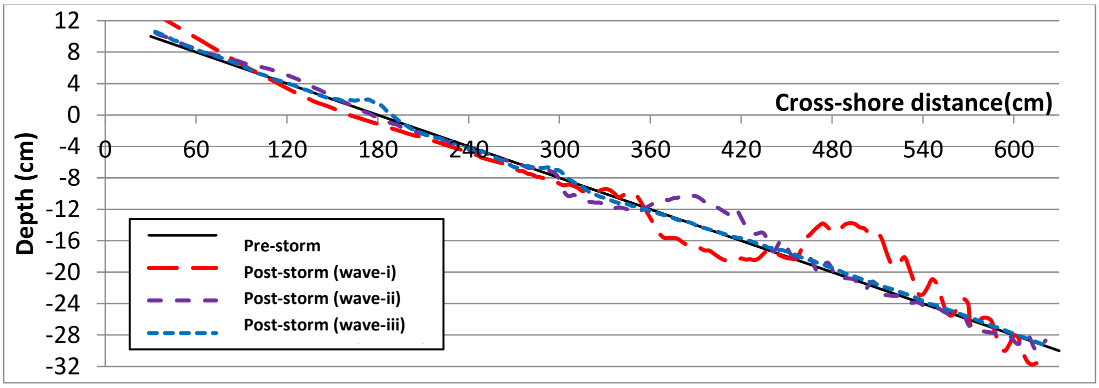

Figure 4.17. Effects of Grain Size, Profile Comparison (Set-1, Top: Fine Sand, Bottom: Coarse Sand)

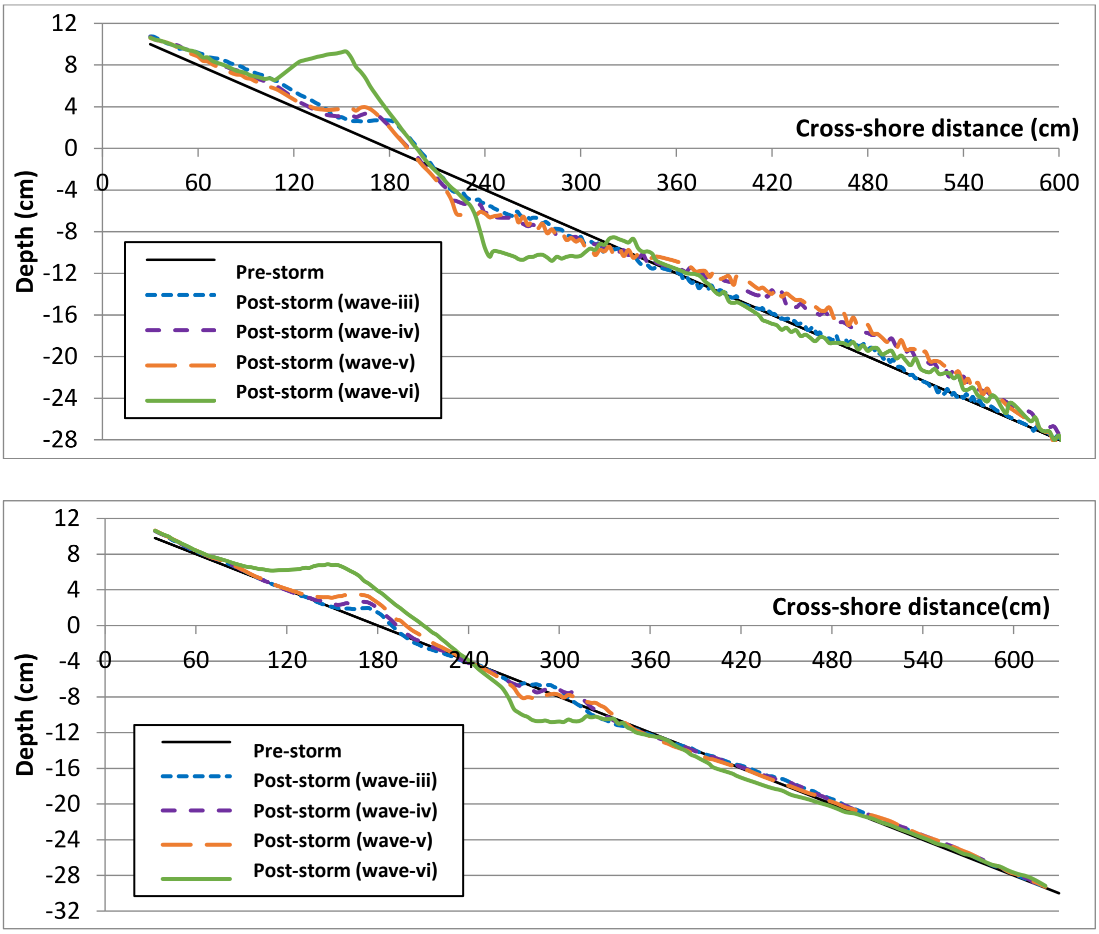

Figure 4.18. Effects of Grain Size, Profile Comparison (Set-2, Top: Fine Sand, Bottom: Coarse Sand)

Table 4.9. Recession(-)/Progression(+) Distances (Prototype Scale) of Stage 2

Wave	D_{50} (mm)	w_s (m/s)	H_s (m)	s_0	α_n	Δy (m)
i	1.3	0.2	3.0	0.04	1:15	-4.0
ii	1.3	0.2	2.0	0.04	1:15	-0.3
iii	1.3	0.2	1.0	0.04	1:15	1.5
iv	1.3	0.2	1.0	0.03	1:15	1.8
v	1.3	0.2	1.0	0.02	1:15	2.4
vi	1.3	0.2	1.0	0.01	1:15	3.0

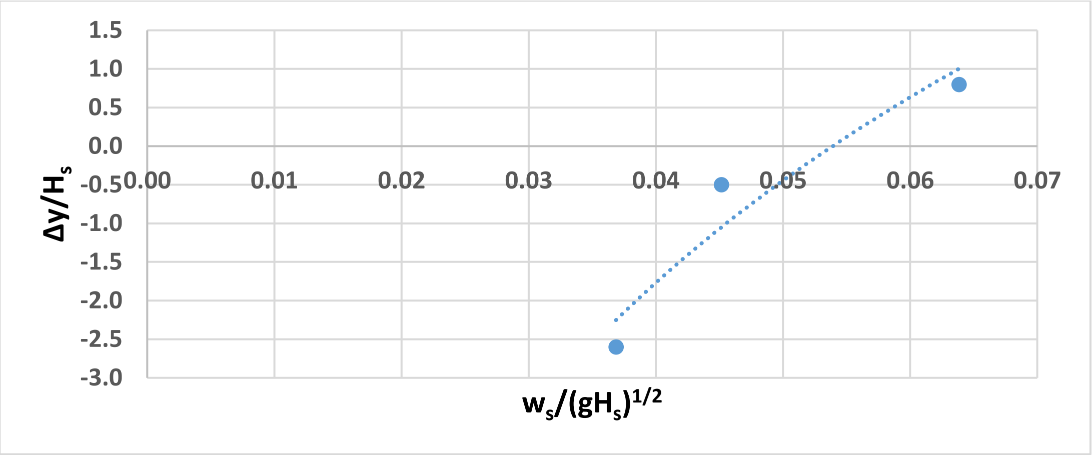

Figure 4.19. Effects of Significant Wave Height (H_s) – s_0=0.04, w_s=0.06 m/s

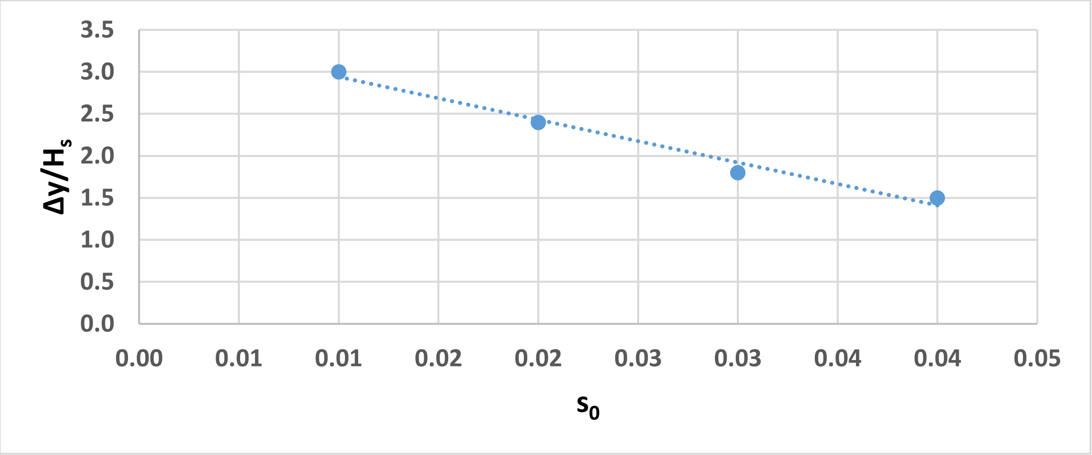

Figure 4.20. Effects of Deep-Sea Wave Steepness (s_0) – H_s=1 m

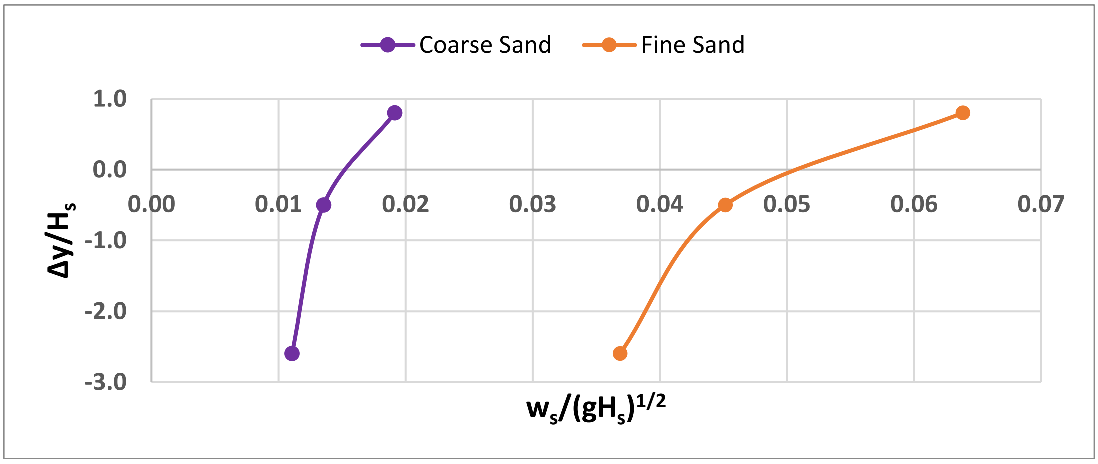

Figure 4.21. Effects of Fall Velocity (w_s) - s_0=0.04

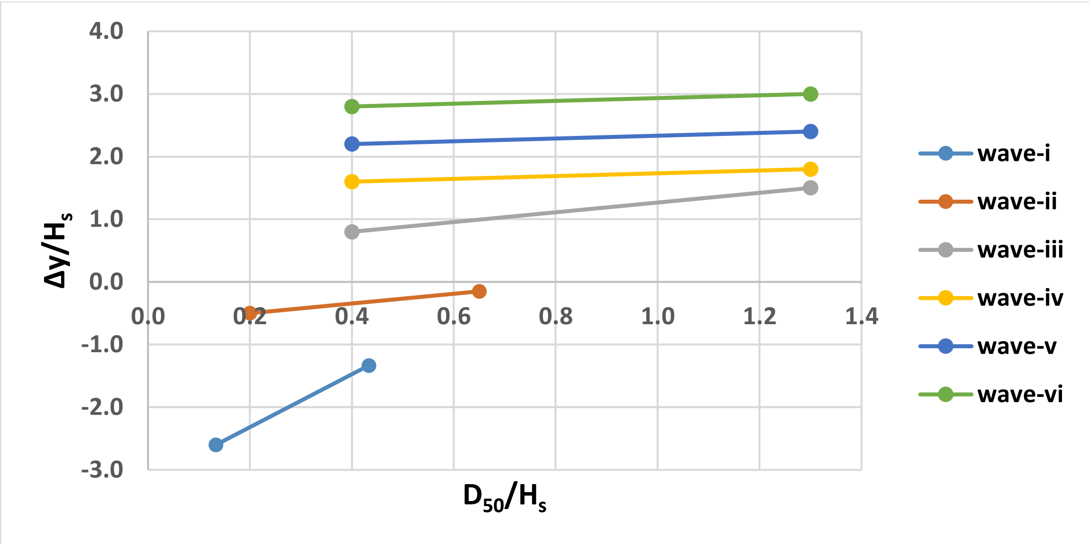

Figure 4.22. Effects of Grain Size (D_{50})

In Table 4.9, Figure 4.19, Figure 4.20 and Figure 4.21, it is seen that when sediment grain diameter increases, recession distances get shorter. Similarly, using bigger grain size affects the beach nourishment positively with a slight increment of accretion distances for accretive waves.

4.4. Beach Fill Slope

In the third stage of experiments, coarse sand is used for beach nourishment having different fill angles. A geotextile tube is placed as a toe structure at a depth of 4 m (0.25 in model scale) and its crest depth is 2.0 m (0.125 m deep in model scale). The dimensions of the geotextile tube (height 2.0 m, diameter 3.25 m in prototype scale) and the materials used are compatible with the field applications. 1:15, 1:10 and 1:5 beach fill slopes under the effects of erosive and accretive waves in the cross-shore bottom profile (Figure 4.23 to 4.27) are examined and given in Figures 4.28, 4.29 and 4.30, respectively. Comparative results between fill slopes are also shown in Figure 4.31. The test parameters used in this stage were given in Table 4.6.

Table 4.10. Stage-3 Experiment Parameters (Model Scale)

Wave	**D_{50} (mm)**	**H_s (cm)**	**s_0**	**d_t (cm)**	**R_c (cm)**	**α_f**	**W_e (cm)**
Winter	0.65	18.75	0.04	25.0	12.5	1:15	120.0
Winter	0.65	18.75	0.04	25.0	12.5	1:10	180.0
Winter	0.65	18.75	0.04	25.0	12.5	1:5	240.0
Summer	0.65	6.25	0.01	25.0	12.5	1:15	120.0
Summer	0.65	6.25	0.01	25.0	12.5	1:10	180.0
Summer	0.65	6.25	0.01	25.0	12.5	1:5	240.0

Figure 4.23. Post-Storm Profile of Accretive Waves Impacting on 1:15 Beach Fill

Figure 4.24. Post-Storm Profile of Erosive Waves Impacting on 1:15 Beach Fill

Figure 4.25. Pre-Storm Profile of 1:5 Beach Fill

Figure 4.26. Post-Storm Profile of Erosive Waves Impacting on 1:5 Beach Fill

Figure 4.27. Post-Storm Profile of Accretive Waves Impacting on 1:5 Beach Fill

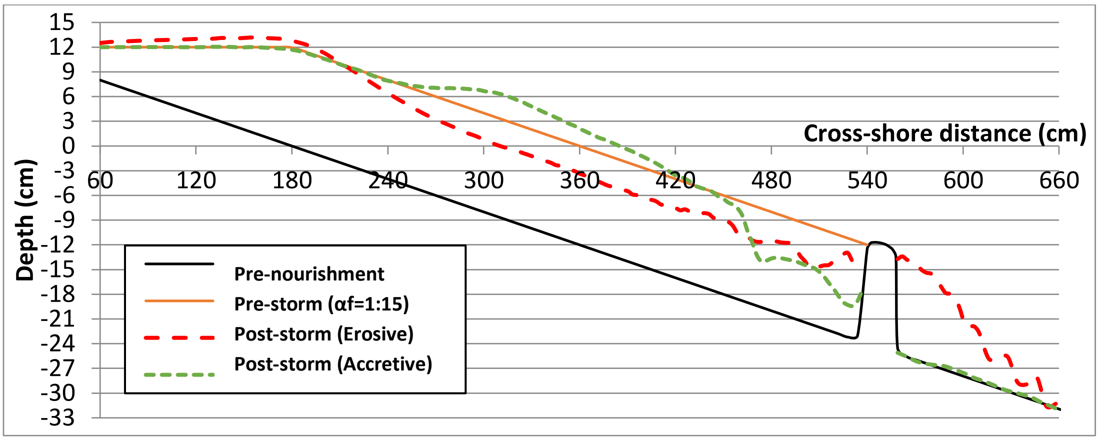

Figure 4.28. Effects of Beach Fill Slope (α_f=1:15)

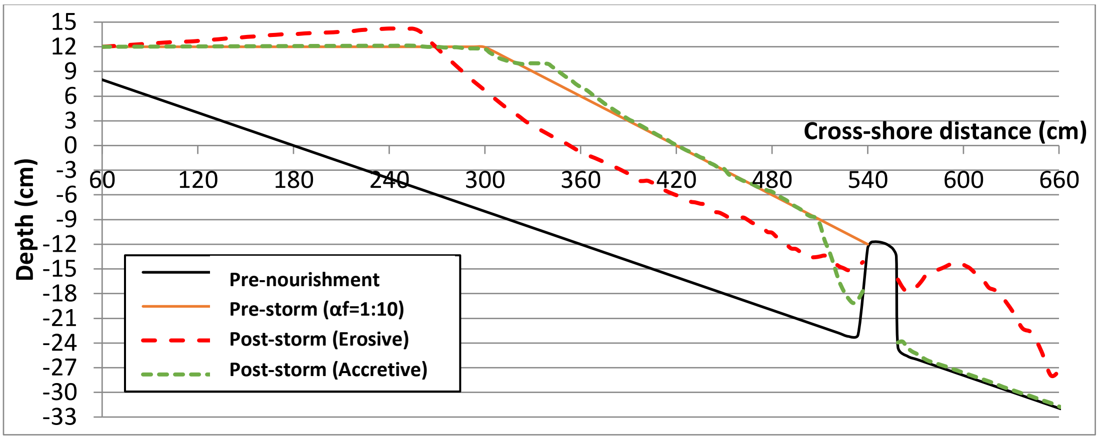

Figure 4.29. Effects of Beach Fill Slope (α_f=1:10)

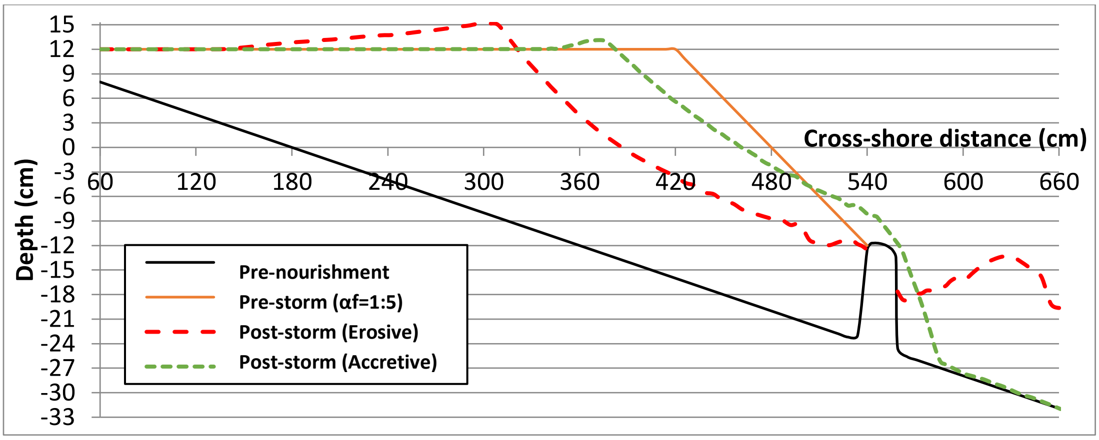

Figure 4.30. Effects of Beach Fill Slope (α_f=1:5)

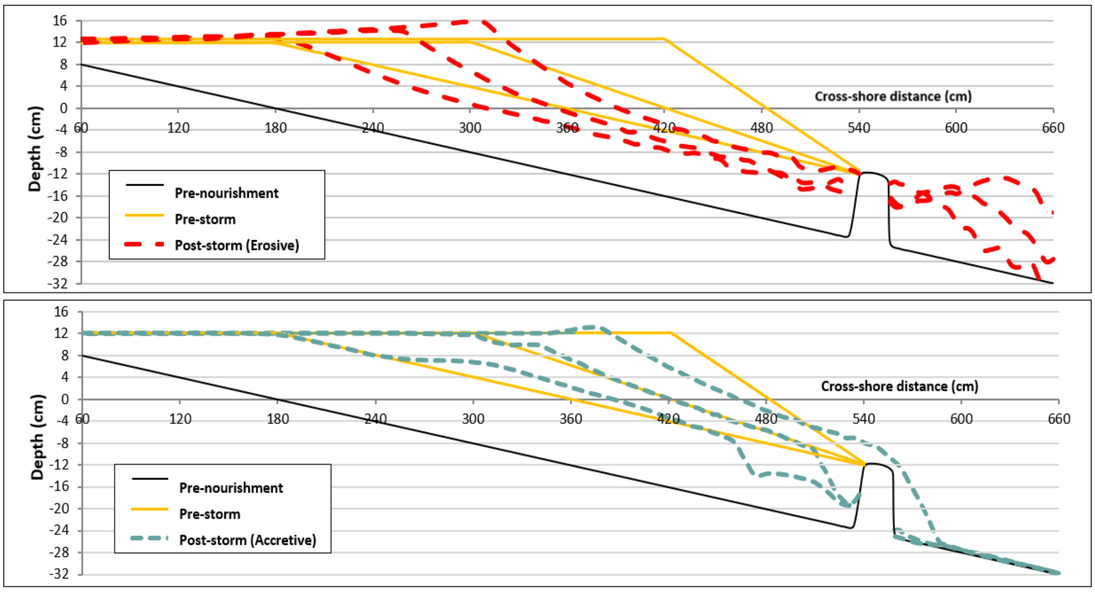

Figure 4.31. Effects of Fill Angle, Profile Comparison (Top: Erosive, Bottom: Accretive Waves)

Table 4.11. Recession(-)/Progression(+) Distances (Prototype Scale) of Stage 3

D_{50} (mm)	H_s (m)	s_0	d_t (m)	R_c (m)	α_f	W_e (m)	Δy (m)
1.3	3.0	0.04	4	2	1:15	19.2	-7.6
1.3	3.0	0.04	4	2	1:10	28.8	-9.9
1.3	3.0	0.04	4	2	1:5	38.4	-14.5
1.3	1.0	0.01	4	2	1:15	19.2	4.9
1.3	1.0	0.01	4	2	1:10	28.8	1.0
1.3	1.0	0.01	4	2	1:5	38.4	-3.0

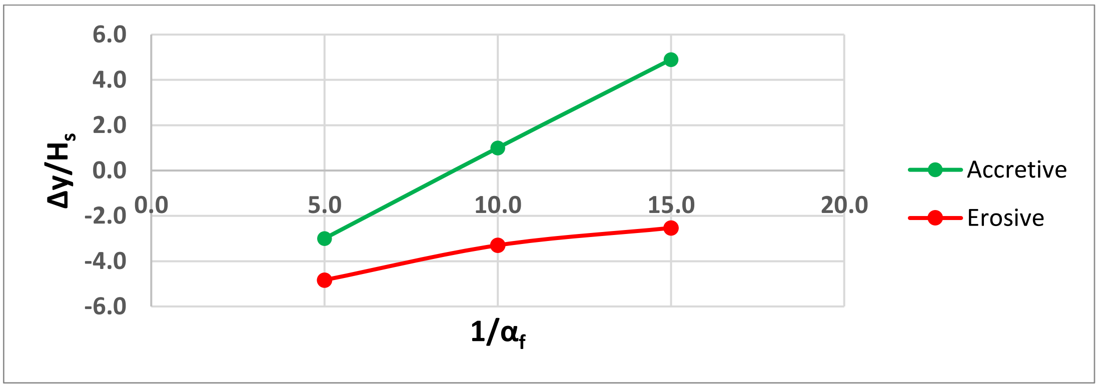

Figure 4.32. Effects of Fill Slope (α_f)

As seen in Figures 4.28 to 4.32 and Table 4.11, when the changes in the bottom profile caused by storm waves in beach nourishment applications carried out with different slopes, it is seen that the geotextile tube placed as a toe structure at a depth of 4.0 m in prototype scale affects the erosion and accumulation wave profiles similarly. The geotextile tube placed in the closure depth of the erosive waves caused scours to be diminished in size with respect to the absence of any toe structure. As the slope of the beach fill getting steeper, the amount of transported sediment and recession distances increase. In the accretive waves, however, the effects are complex. The geotextile tube outside the breaking zone broke the waves with the effect of the crest depth and caused large scours just behind the structure. As the beach fill angle getting steeper, it reduces the distance between the depth of closure and the toe structure and the amount of sand, the amount of transported sediment and accretion distances caused by breaking waves on the structure reduce. In the last experiment with a beach fill slope of 1:5, the toe structure is buried under the sand. By looking at the figures, it can be said that bottom profile gets steeper, recession distances increase for erosive waves. Similar effects are applicable for accretive waves; in fact, if bottom slope is too steep, accretion efficiency of summer waves decreases, they even become erosive.

4.5. Location and Dimensions of Geotextile Tubes

Fourth stage of the experiments is about the location (depth) of the geotextile tube. Only the position of the tube and its dimensions are changed by moving it outside the wave breaking zone, other variables such as sand grain diameter are kept constant (Table 4.12). Post-storm profiles are drawn, and recession distances were compared. After the same geotextile tube was placed as a toe structure at a depth of 6.0 m (outside the breaking zone) in a prototype scale, the effects of the waves eroding and accreting on a beach fill with a slope of 1:10 can be seen in Figure 4.33, and in order to get the same crest depth (R_c=2.0m) as in Stage-3. the size of the geotextile tube is doubled (height is 4.0 m, diameter is 6.5 m on prototype scale). Then experiments of both storms are repeated and the resulting bottom profiles are given in Figure 4.35 and 4.36.

Table 4.12. Stage-4 Experiment Parameters (Model Scale)

Wave	D_{50} (mm)	H_s (cm)	s_0	d_t (cm)	R_c (cm)	α_f	W_e (cm)
Winter	0.65	18.75	0.04	37.5	25.0	1:10	180.0
Winter	0.65	18.75	0.04	37.5	12.5	1:10	180.0
Summer	0.65	6.25	0.01	37.5	25.0	1:10	180.0
Summer	0.65	6.25	0.01	37.5	12.5	1:10	180.0

Figure 4.33. Post-Storm Profile of Erosive Waves Impacting on Large Submerged Breakwater

Figure 4.34. Post-Storm Profile of Erosive Waves Impacting on Small Submerged Breakwater

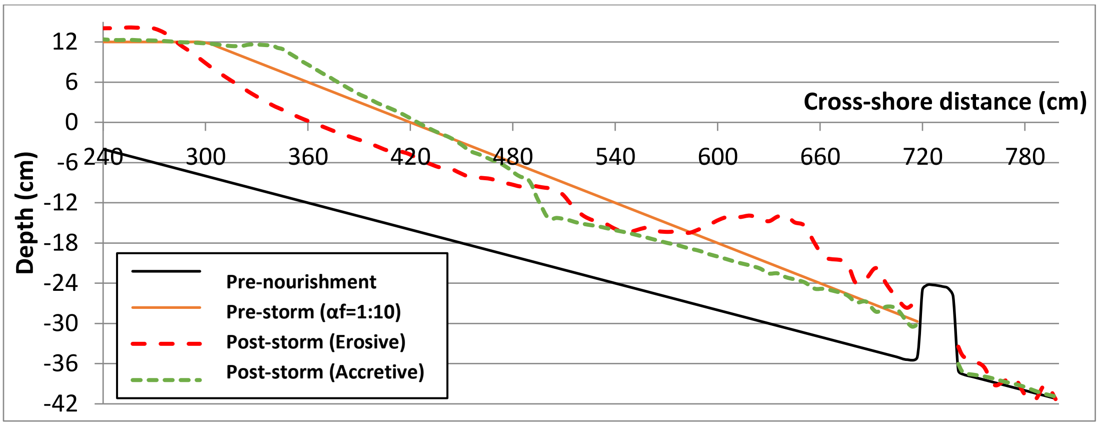

Figure 4.35. Effects of Location of Geotextile Tube

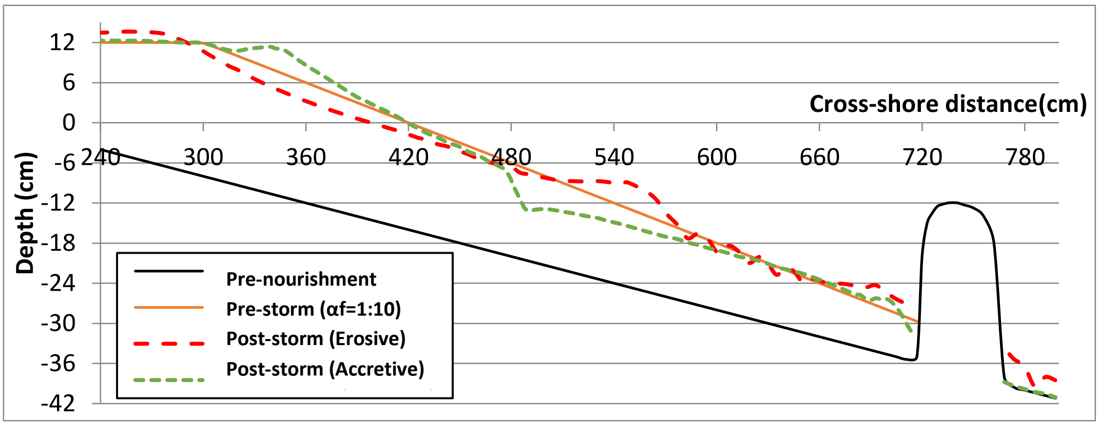

Figure 4.36. Effects of Crest Depth (R_c)

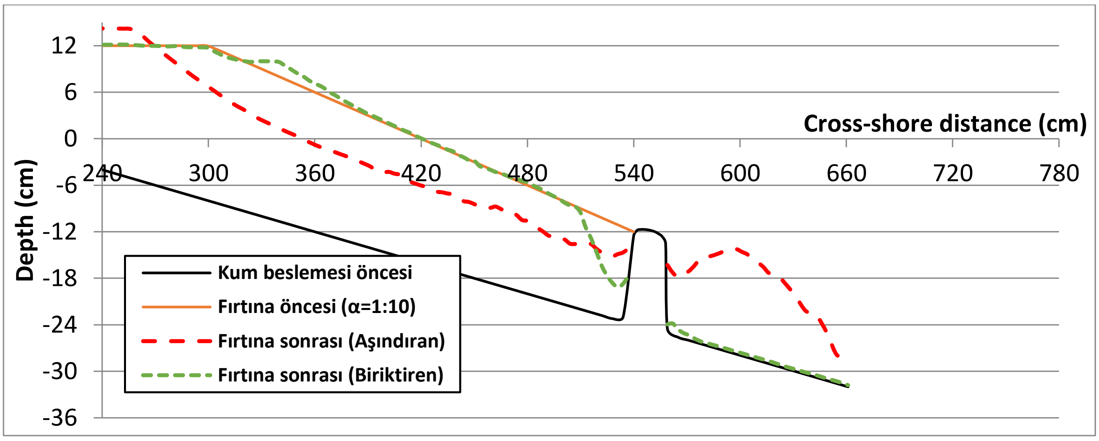

Figure 4.37. Effects of Toe Depth of Structure (d_t)

Table 4.13. Recession(-)/Progression(+) Distances (Prototype Scale) of Stage 4

D_{50} (mm)	H_s (m)	s_0	d_t (m)	R_c (m)	α_f	W_e (m)	Δy (m)
1.3	3.0	0.04	4	2	1:10	28.8	-9.9
1.3	3.0	0.04	6	4	1:10	28.8	-9.2
1.3	3.0	0.04	6	2	1:10	28.8	-3.5
1.3	1.0	0.01	4	2	1:10	28.8	1.0
1.3	1.0	0.01	6	4	1:10	28.8	0.7
1.3	1.0	0.01	6	2	1:10	28.8	-0.1

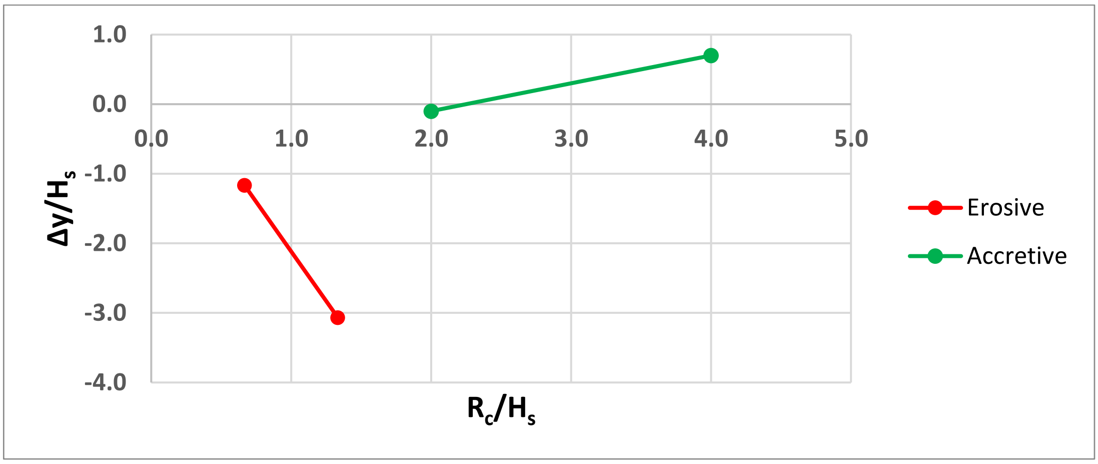

Figure 4.38. Effects of Fill Slope (α_f)

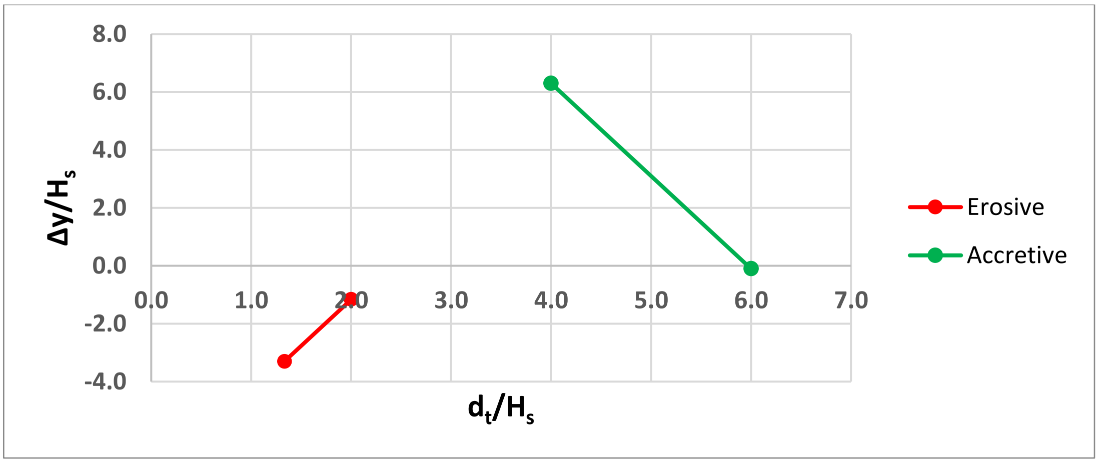

Figure 4.39. Effects of Fill Slope (α_f)

By looking at Figure 4.35 to 4.39 and Table 4.13, it was found that the geotextile tubes work more efficiently when they placed near closure depth instead of the breaking zone. It has been measured that the scours and ripples caused by the breaking waves are reduced, the sediment movement decreases nearshore and consequently the recession distances are reduced. For the accreting waves, as the distance between the closure depth and toe structure increased, only the bottom profile in the area just behind the toe structure is changed and there is no significant change in the shoreline.

When a larger geotextile tube is placed at the same depth, the contribution of the toe structure which works as a submerged breakwater to the wave transmission is become very useful and accordingly the shoreline changed in a positive way. No significant change is observed in the profile of the accretive waves, yet for erosive waves, the volume of eroded regions decreased significantly due to low wave transmission and breaking. This is also a result of wide crest of submerged breakwater. Due to the height of toe structure, the trapped sand amount increases, keeping the applied beach fill on the shore, and reducing the recession distances. That shows the geotextile tube performs better when placed outside of the breaking zone as a submerged breakwater.

4.6. Depth and Presence of Toe Structure

In the final stage of the experiments, no toe structure is used, geotextile tubes are removed from the channel. The same sand fill is used with a slope of 1:10 until it is intersected with a natural bottom profile with a constant slope of 1:15. The effects of the waves without any toe protection structure can be seen in Figure 4.40. The parameters used were given in Table 4.14.

Table 4.14. Stage-5 Experiment Parameters (Model Scale)

Wave	D_{50} (mm)	H_s (cm)	s_0	d_t (cm)	R_c (cm)	α_f	W_e (cm)
Winter	0.65	18.75	0.04	-	-	1:10	180.0
Summer	0.65	6.25	0.01	-	-	1:10	180.0

Figure 4.40. Post-Storm Profile of 1:10 Beach Fill without a Toe Structure

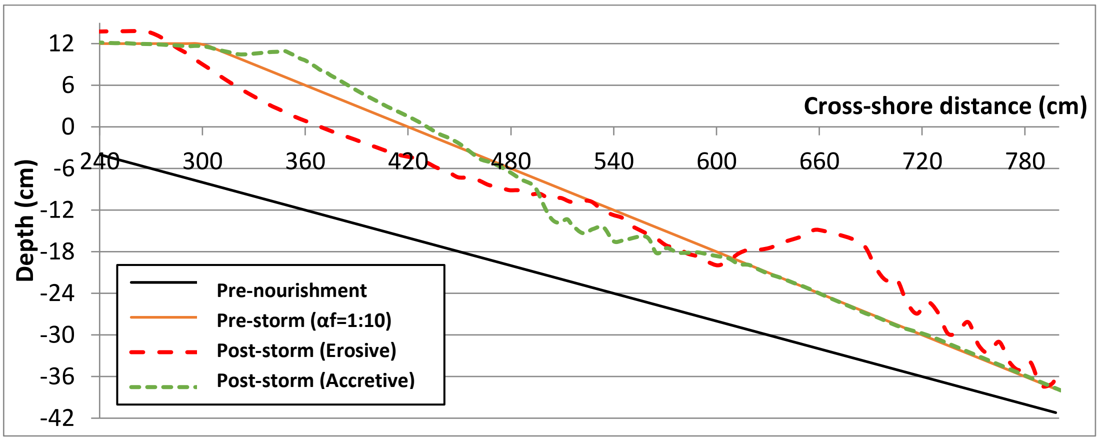

Figure 4.41. Effects of Presence of Toe Structure

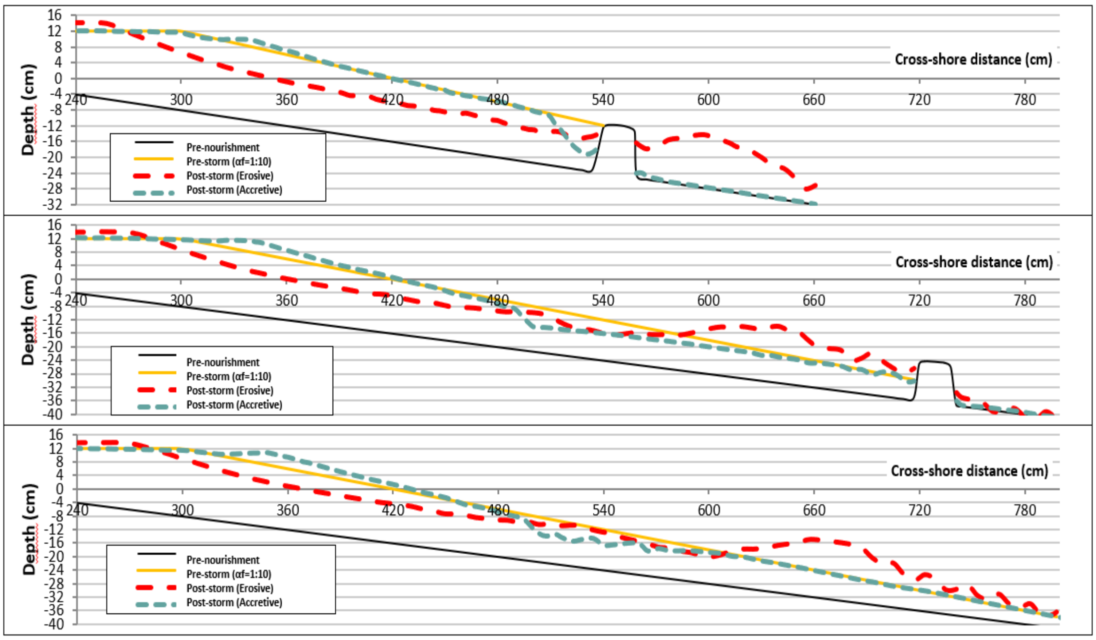

Figure 4.42. Effects of Depths and Presence of Toe Structure, Profile Comparison

Table 4.15. Recession(-)/Progression(+) Distances (Prototype Scale) of Stage 5

D_{50} (mm)	H_s (m)	s_0	d_t (m)	R_c (m)	α_f	W_e (m)	Δy (m)
1.3	3.0	0.04	-	-	1:10	28.8	-8.2
1.3	1.0	0.01	-	-	1:10	28.8	1.8

The absence of toe structure in the accretive waves leads to the formation of sand bars nearshore, but no significant change in the sand volumes accumulated on the shore. The absence of toe structure in erosive waves, however, causes the sand bars to form deeper, but no significant changes were observed in the eroded sand volumes on the shore. As a result of these experiments, toe structures placed in the breaking zone did not have a positive effect on the post-storm bottom profile and it was observed that the geotextile tubes placed outside the breaking zone worked more efficiently. For a detailed performance analysis, along the recession distances on the shoreline, the sand fill volumes, the volumes of scours and bars formed, and the volumes of sand escapes to deep which cannot be returned must be calculated by numerical models.

4.7. Efficiency of Beach Nourishment

The recession/progression distances (Δy) and efficiency ratios of beach fills, $(W_e+\Delta y)/W_e$, are summarized in Table 4.16 and Table 4.17. In the tables, if $(W_e+\Delta y)/W_e<1$, recession of shoreline is the case, otherwise there will be progression on the shoreline. In both tables, all values are given on the prototype scale.

Table 4.16. Efficiency Ratio of Beach Fills (Prototype Scale) – Experiment Stage 3

D_{50} (mm)	H_s (m)	s_0	d_t (m)	R_c (m)	α_f	W_e (m)	Δy (m)	$(W_e+\Delta y)/W_e$
1.3	3.0	0.04	4	2	1:15	19.2	-7.6	0.60
1.3	3.0	0.04	4	2	1:10	28.8	-9.9	0.66
1.3	3.0	0.04	4	2	1:5	38.4	-14.5	0.62
1.3	1.0	0.01	4	2	1:15	19.2	4.9	1.26
1.3	1.0	0.01	4	2	1:10	28.8	1.0	1.03
1.3	1.0	0.01	4	2	1:5	38.4	-3.0	0.92

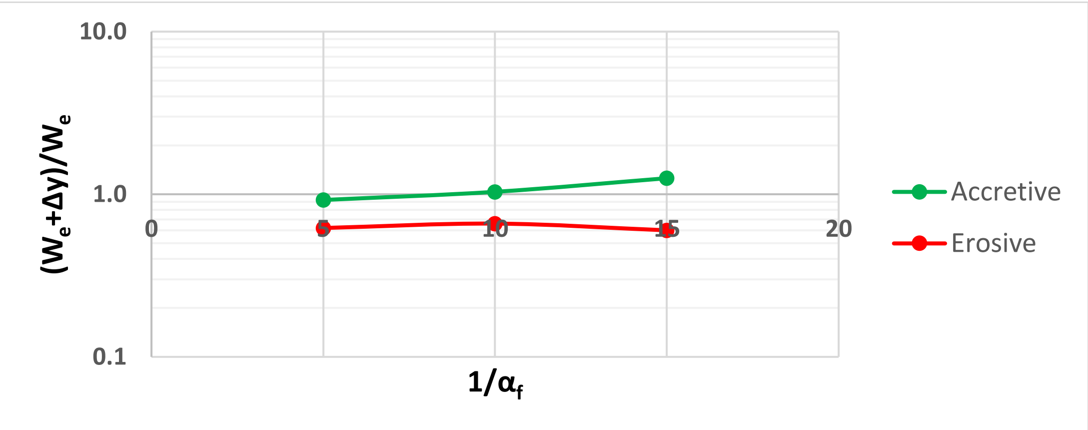

Figure 4.43. Effects of Bottom Slope (α_f) – Efficiency Ratio

According to Figure 4.43, as the bottom profile gets steeper, recession distances increase. Similar effects are applicable for accretive waves; in fact, if bottom slope is too steep, accretion efficiency of summer waves decreases, they even become erosive.

Table 4.17. Efficiency Ratio of Beach Fills (Prototype Scale) – Experiment Stage 4-5

D_{50} (mm)	H_s (m)	s_0	d_t (m)	R_c (m)	α_f	W_e (m)	Δy (m)	$(W_e+\Delta y)/W_e$
1.3	3.0	0.04	6	4	1:10	28.8	-9.2	0.68
1.3	3.0	0.04	6	2	1:10	28.8	-3.5	0.88
1.3	3.0	0.04	-	-	1:10	28.8	-8.2	0.72
1.3	1.0	0.01	6	4	1:10	28.8	0.7	1.02
1.3	1.0	0.01	6	2	1:10	28.8	-0.1	1.00
1.3	1.0	0.01	-	-	1:10	28.8	1.8	1.06

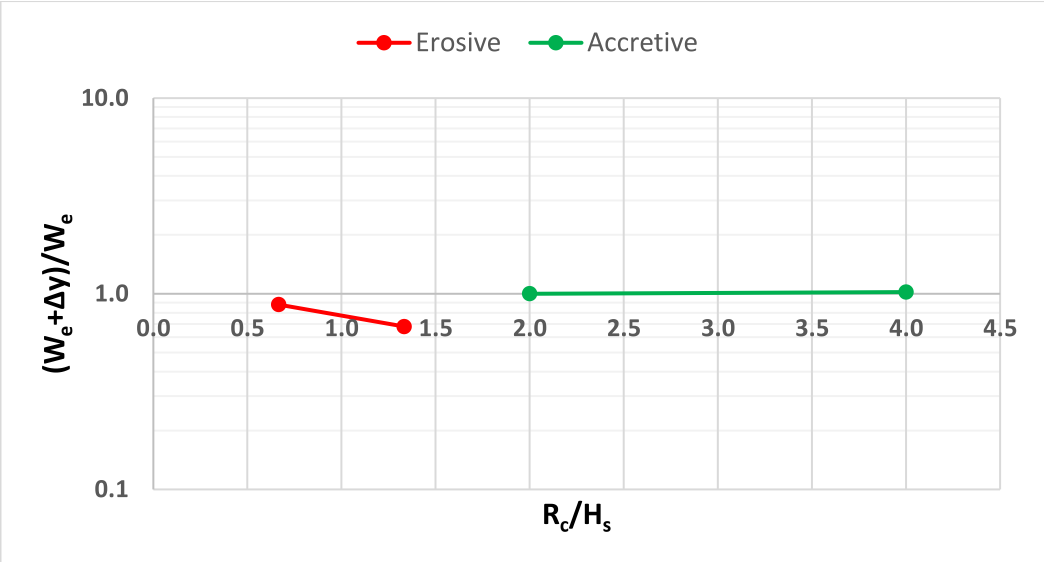

Figure 4.44. Effects of Crest Depth (R_c) – Efficiency Ratio

By looking at Figure 4.44, it can be commented that using bigger structure (i.e. shallower structure crest) at the same depth reduces erosion rates substantially. For smaller wave heights, such as summer waves, however, the effects are almost negligible since waves are not being influenced by both submerged breakwaters.

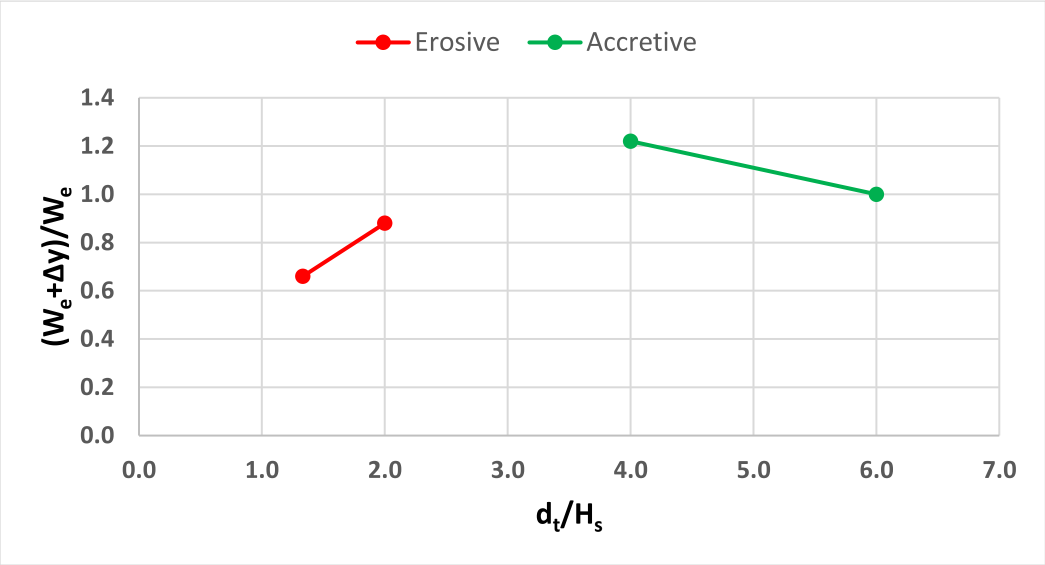

Figure 4.45. Effects of Toe Depth (d_t) – Efficiency Ratio

According to Figure 4.45, using bigger structure before breaking depth increases the efficiency of beach nourishment and decreases the recession distance. One of the reasons of that is width of submerged breakwater is double of toe structure, so wave breaking rates are higher. In other words, the waves that cause erosion break earlier and become ineffective nearshore. Yet, like the previous case, accretive waves cannot be affected by geotextile tubes and almost no change is observed on the shoreline..

CHAPTER 5

CONCLUSION AND FUTURE RECOMMENDATIONS

In this study, the performance of submerged geotextile structures as toe protection in beach nourishment applications is investigated through physical model tests. Sand protection rates and performances of geotextile tubes are evaluated according to bottom profile changes (erosion/accretion) due to cross-shore sediment transport and post-storm recession of the shoreline. The results obtained after the physical model experiments and measurements are summarized below.

1. While other variables are constant and significant wave height and/or wave steepness increases, sediment moves towards offshore and recession distances increase. While steep (storm) waves erode, calm (swell) waves deposit the sand.

2. It has been observed that as the grain sizes increase, the sediment movement nearshore and recession distances decrease. That is why a beach nourishment application using coarser sand than the natural becomes more efficient.

3. In the experiments where the geotextile tube is applied as toe protection, while the angle of the beach fill getting steeper, sediment transport and recessions increase. This phenomenon is based on the increasing volume of the filled sand and extended berm width. Sediment grain which has moved towards offshore cannot return nearshore after it passes through the toe structure or closure depth.

4. Placing the geotextile tube outside the breaking zone and making it work as a submerged breakwater increases the efficiency of the beach nourishment. Waves that cause erosion gets smaller by breaking before even reaching the surf zone, and their energy is lost due to low wave transmission rates of wide submerged breakwaters.

5. During the beach nourishment application, the toe structure placed in the surf zone increases the accumulated sand on the shoreline, under the effect of accretive waves. For erosive waves, however, the toe structure causes nearshore agitation and slight increment can be seen in the recession distances.

For a detailed performance analysis of geotextile tubes, sediment volumes moved in front of and behind the toe structure, scour depths, bar formations, ripple heights and lengths should be assessed by numerical modeling and included in the evaluation process, in addition to measurements of shoreline recession or progression distances and filled/eroded sand volumes.

In the light of the obtained results and experimental data, it will be possible to calibrate different numerical models, and the number of variables compared can be increased. Therefore, more detailed measurements and comparisons can be prepared. Flow and wave parameters such as velocities around geotextile tubes can be assessed and modeled. By doing that, wave transmission, stability and scour concerns can be satisfied before implementing a geotextile tubes as a toe protection or a submerged breakwater. As a result of this study, it is aimed to find ideal conditions and variables in the use of geotextile tubes in beach nourishment applications. Detailed design and modeling processes in beach nourishment have great importance for the success of the application, in order to get the best efficiency on the nourished beaches.

REFERENCES

Bağcıoğlu, E. (2001). Kıyı yenileme çalışmalarının genel karakteristiklerinin araştırılması [In Turkish]. MSc Thesis Balikesir University, Graduate School of Natural and Applied Sciences, Turkey.

Baykal, C., Tarakcıoğlu, G.Ö., Işık, E., Güler, H.G., Aydın, D.C., Çınar, G.E., Yalçıner, A.C., Güler, I. and Ergin, A. (2017). Application of XBeach in a beach nourishment and restoration project, a case study: Alanya-Türkler, Turkey. XBeach X Users Conference. Delft, The Netherlands.

Bezuijen, A. and Vastenburg, E.W. (2012). Geosystems: Design Rules and Applications. CRC Press.

Birkemeier, W.A. (1985). Field data on seaward limit of profile change. Journal of Waterway, Port, Coastal and Ocean Engineering 111(3), 598-602.

Bolle, A., Mercelis, P., Roelvink, D., Haerens, P. and Trouw, K. (2010). Application and validation of XBeach for three different field sites. In Proceedings of the Coastal Engineering Conference.

Bruun, P. (1954). Coast erosion and the development of beach profiles, Technical Memorandum No. 44, Beach Erosion Board. U.S. Army Corps of Eng.

Chatham, C.E. (1972). Movable-bed model studies of perched beach concept. Proc. 13th Coastal Engineering Conference (Vancouver), 2, 1197–1216.

CUR (1990). Manual on Artificial Beach Nourishment, CUR Rep. 130, Balkema Press, Rotterdam.

Dalrymple, R.A. and Thompson, W.W. (1976). Study of equilibrium beach profiles. Proceedings of the Fifteenth Coastal Engineering Conference, July 11-18, Honolulu, HI, ASCE, New York: 1277-1296.

das Neves, L. (2011). Experimental stability analysis of geotextile encapsulated-sand systems under wave-loading. PhD Thesis University of Porto, Faculty of Engineering, Portugal.

das Neves, L., Moreira, A., Taveira-Pinto, F., Lopes, M.L. and Veloso-Gomes, F. (2015). Performance of submerged nearshore sand-filled geosystems for coastal protection. Coastal Engineering, 95, 147–159.

De Carlo, M., Yates, M., van Bang, D.P., Gervais, M. and Vidal, V. (2017). Evaluating storm erosion with XBeach on beaches protected by submerged structures. XBeach X Users Conference. Delft, The Netherlands.

Dean, R.G. (1977). Equilibrium beach profiles: U.S. Atlantic and Gulf Coasts. Ocean Engineering Technical Report No. 12, Department of Civil Engineering and College of Marine Studies, University of Delaware.

Dean, R.G. (1987). Additional sediment input to the nearshore region. Shore and Beach, 55(3-4), 76-81.

Dean, R.G. (1991). Equilibrium beach profiles: characteristics and applications. Journal of Coastal Research, 7(1), 53–84.

Dean, R.G. (2002). Beach Nourishment: Theory and Practice, World Scientific Press, New Jersey.

Dean, R.G. (2005). Beach nourishment: benefits, theory and case examples, In: Zimmermann, C.; Dean, R.G.; Penchev, V. and Verhagen, H.J. (eds.), Environmentally Friendly Coastal Protection. Netherlands: Springer, 25–40.

Dean, R.G. and Dalrymple, R.A. (2001). Coastal Processes with Engineering Applications. Cambridge University Press.

Faraci, C. (2018). Experimental investigation of the hydro-morphodynamic performances of a geocontainer submerged reef. Journal of Waterway, Port, Coastal, and Ocean Engineering, 144(2).

Giardino, A., Broekema, Y., van der Werf, J., Rooijen, A.V., Vousdoukas, M.I. (2015). IAHR World Congress, Vol. 36. The Hague, The Netherlands.

Goda, Y. (2010). Random Seas and Design of Maritime Structures. In Advanced Series on Ocean Engineering, Vol. 33, 1–732.

Goda, Y. and Suzuki, Y. (1977). Estimation of incident and reflected waves in random wave experiments. In Proc. Fifteenth Coastal Eng. Conf. (Hawaii Univ. U.S.A.), 1, New York, U.S.A. American Soc. Civ. Eng.

González, M., Medina, R. and Losada, M.A. (1999). Equilibrium beach profile model for perched beaches. Coastal Engineering, 36(4), 343–357.

Gourlay, M.R. (1968). Beach and dune erosion tests, Delft Hydraulics Laboratory, Report No. M935/M936.

Hallermeier, R.J. (1978). Uses for a calculated limit depth to beach erosion. Proceedings, 16th Coastal Engineering Conference, American Society of Civil Engineers, 1493- 15 12.

Hanson, H. and Kraus, N.C. (1989). GENESIS: generalized model for simulating shoreline change. Report 1: technical reference. Technical Report - US Army Coastal Engineering Research Center, 89–19.

Hanson, H., Brampton, A., Capobianco, M., Dette, H., Hamme, L., Laustrup, C., Lechuga, A. and Spanhoff, R. (2002). Beach nourishment projects, practices, and objectives a European overview, Coastal Engineering, vol. 47, 81-111.

Hughes, S.A. (1983). Movable bed modeling law for coastal dune erosion. Journal of Waterway, Port, Coastal and Ocean Engineering, 109(2), 164-179.

Hughes, S. (1993). Physical Models and Laboratory Techniques in Coastal Engineering, Vol. 7, World Scientific, Singapore.

Koerner, R.M. (2016). Geotextiles: From Design to Applications. Elsevier Ltd.

Kuang, C., Pan, Y., Zhang, Y., Liu, S., Yang, Y., Zhang, J. and Dong, P. (2011). Performance evaluation of a beach nourishment project at West Beach in Beidaihe, China. (2011). Journal of Coastal Research, 27(4), 769.

Larson, M. and Kraus, N.C. (1989). SBEACH: numerical model for simulating storm-induced beach change; report 1: empirical foundation and model development. Technical Report - US Army Coastal Engineering Research Center, 89–9.

Lawson, C.R. (2008). Geotextile containment for hydraulic and environmental engineering. Geosynthetics International, 15(6), 384–427.

Moore, B.D. (1982). Beach profile evolution in response to changes in water level and wave height. Master’s Thesis, Department of Civil Engineering, University of Delaware.

Nordstrom, K.F. (2008). Beach and Dune Restoration. Cambridge University Press.

Oh, Y.I. and Shin, E.C. (2006). Using submerged geotextile tubes in the protection of the E. Korean shore. Coastal Engineering, 53(11), 879–895.

Oumeraci, H. and Recio, J. (2017). Geotextile sand containers for shore protection. In Handbook of Coastal and Ocean Engineering: Expanded Edition (Vol. 1–2, 775–822). World Scientific Publishing Co. Pte. Ltd.

Pilarczyk, K.W. (1995). Novel Systems in Coastal Engineering; Geotextile Systems and Other Methods. Rijkswaterstaat, Delft, the Netherlands.

Recio, J. and Oumeraci, H. (2009). Process based stability formulae for coastal structures made of geotextile sand containers. Coastal Engineering, 56(5–6), 632–658.

Roelvink, D., Reniers, A., van Dongeren, A., van Thiel de Vries, J., McCall, R. and Lescinski, J. (2009). Modelling storm impacts on beaches, dunes and barrier islands. Coast. Eng. 56 (11–12), 1133–1152.

Shin, E.C. and Oh, Y.I. (2005). The stability and wave transmit analysis of submerged geotextile tube breakwater by hydraulic model test. In Proceedings of the International Offshore and Polar Engineering Conference. 525–530.

Stokes, G.G. (1851). On the effect of internal friction of fluids on the motion of pendulums. Transactions of the Cambridge Philosophical Society. 9-ii: 8-106.

Sorensen, R.M. (2006). Basic Coastal Engineering, 3rd ed. Berlin: Springer.

Sorensen R.M. and Beil, N.J. (1988). Perched beach profile response to wave action. Proc. 21st. International Conference on Coastal Eng. ASCE, 1482-1491.

Swart, D.H. (1974). A schematization of onshore-offshore transport. Proceedings of the Fourteenth International Conference on Coastal Engineering, American Society of Civil Engineers, 884-900.

Tayade, B.R., Mahalingaiah, A.V., Gokhale, N.V. and Kudale, M.D. (2015). Importance of location & alignment of geotextile tubes for the coastal protection measures. Aquatic Procedia, 4, 190–197.

US Army, Corps of Engineers (1984). Shore Protection Manual, Vol. 1. Coastal Engineering Research Center.

van Rijn, L.C. (2014). A simple general expression for longshore transport of sand, gravel and shingle. Coastal Engineering, 90, 23–39.

van Rijn, L.C., Tonnon, P.K. and Walstra, D.J.R. (2011). Numerical modelling of erosion and accretion of plane sloping beaches at different scales. Coastal Engineering, 58(7), 637–655.

van Steeg, P. and Bezuijen, A. (2010). Large scale physical model tests on sand filled geotextile tubes and containers. In 9th International Conference on Geosynthetics - Geosynthetics: Advanced Solutions for a Challenging World, 1221–1224. Brazilian Chapter of the International Geosynthetics Society.

van Steeg, P., Vastenburg, E., Bezuijen A., Zengerink, E. and de Gijt, J. (2011). Large-scale physical model tests on sand-filled geotextile tubes and containers under wave attack. Proc. of the 6th Int. Conf. on Coastal Structures, Japan Society of Civil Engineers.

Wright, L.D. and Short, A.D. (1984). Morphodynamic variability of surf zones and beaches. Mar. Geol. 56, 93–118.

Yalçıner A.C., Ergin A., Pamukçu S. and Derun B.A. (2004). Performance of perforated breakwaters constructed with geotextile tubes. Journal of Coastal Research, 39, 750-753

Zimmermann, N., Trouw, K., De Maerschalck, B., Toro, F., Delgado, R., Verwaest, T. and Mostaert, F. (2015). Scientific support regarding hydrodynamics and sand transport in the coastal zone. Technical Report, Flanders Hydraulic Research., 57.

APPENDICES

A. PHOTOGRAPHS FROM PHYSICAL MODEL EXPERIMENTS

Figure A.1. Ripples Due to Wave-(ii) (Hs=2m and s=0.04)

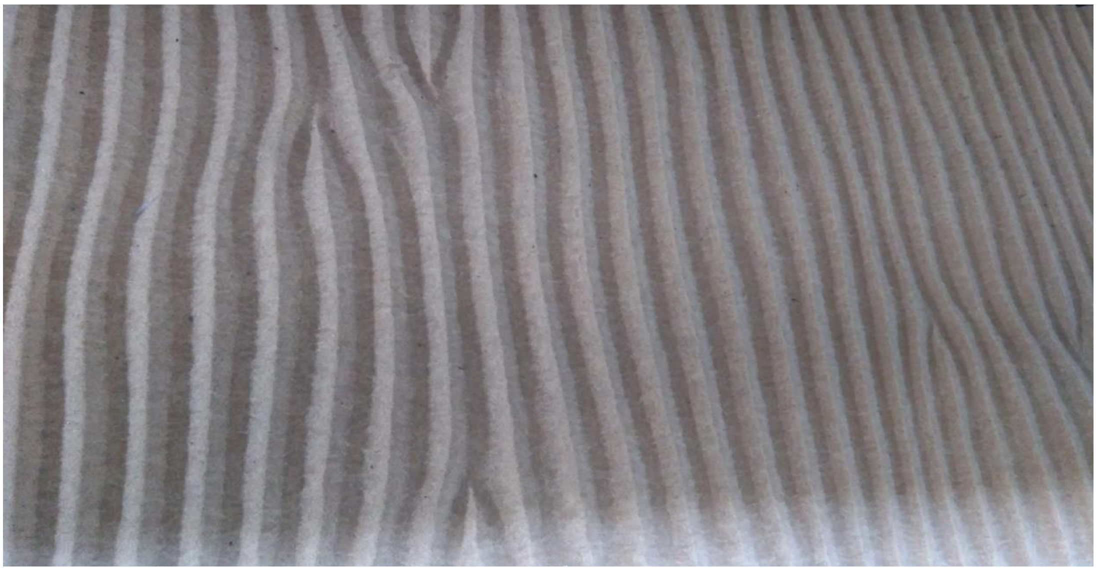

Figure A.2. Ripples Due to Wave-(iii) (Hs=1m and s=0.04)

Figure A.3. Ripples Due to Wave-(iv) (Hs=1m and s=0.03)

Figure A.4. Sand Berm Due to Wave-(v) (Hs=1m and s=0.02)

Figure A.5. Ripples Due to Wave-(vi) (Hs=1m and s=0.01)

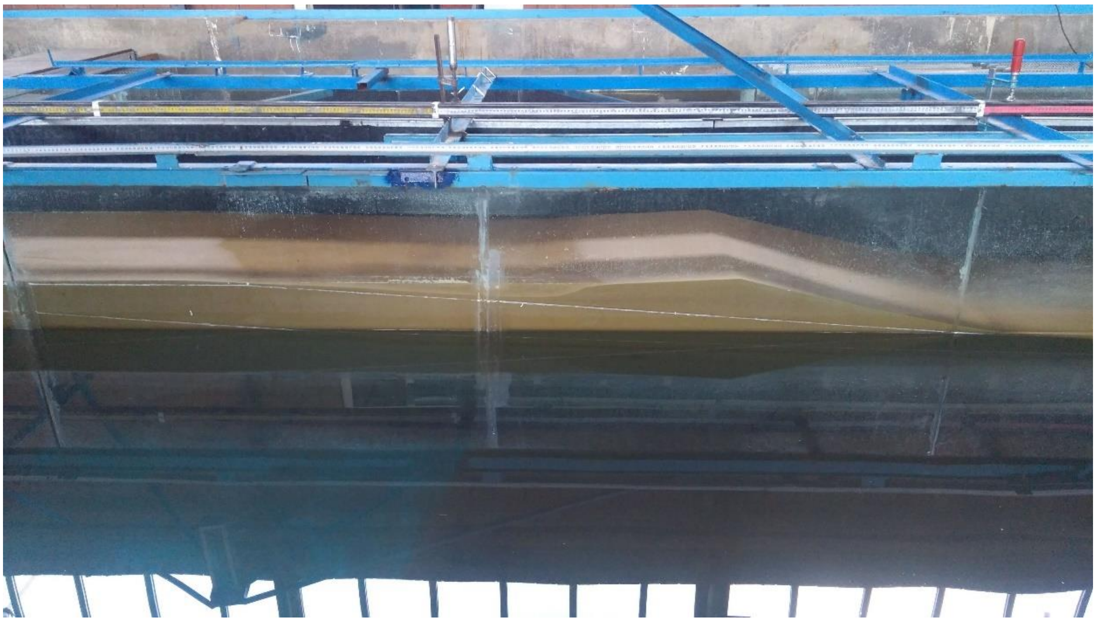

Figure A.6. Post-Storm Bottom Profile of Accretive Waves onto 1:15 Beach Fill

Figure A.7. Sand Berm and Bottom Profile of Summer Waves Acting on 1:15 Beach Fill

Figure A.8. Post-Storm Bottom Profile of Erosive Waves onto 1:15 Beach Fill

Figure A.9. Post-Storm Scour Around Geotextile Tube

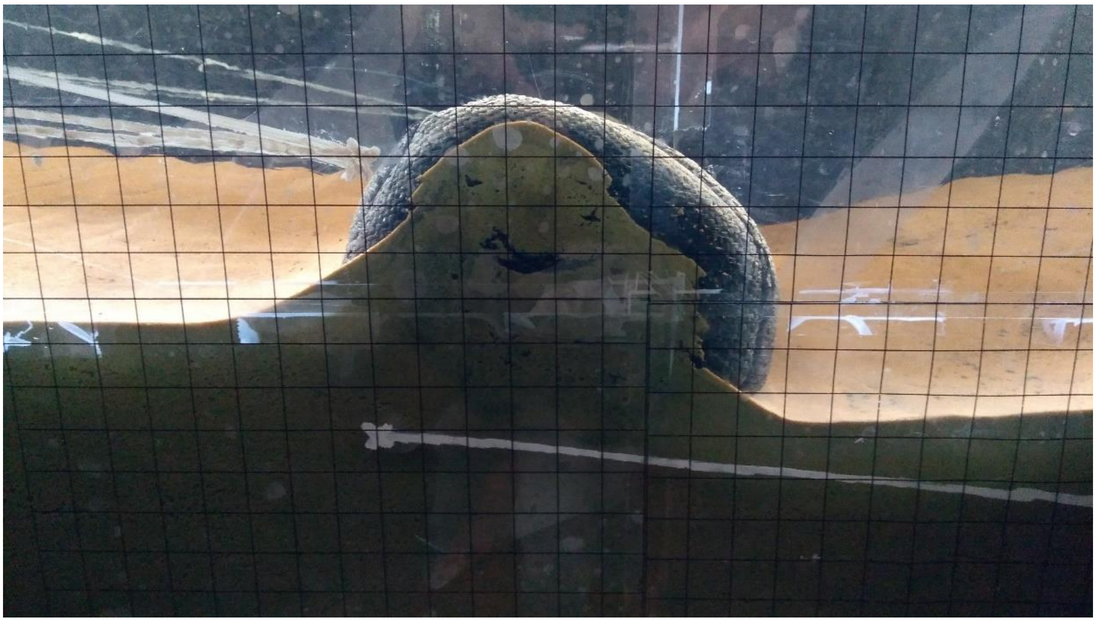

Figure A.10. Post-Storm Erosion and Scour Around Geotextile Tube

Figure A.11. Post-Storm Bottom Profile of Erosive Waves onto 1:15 Beach Fill

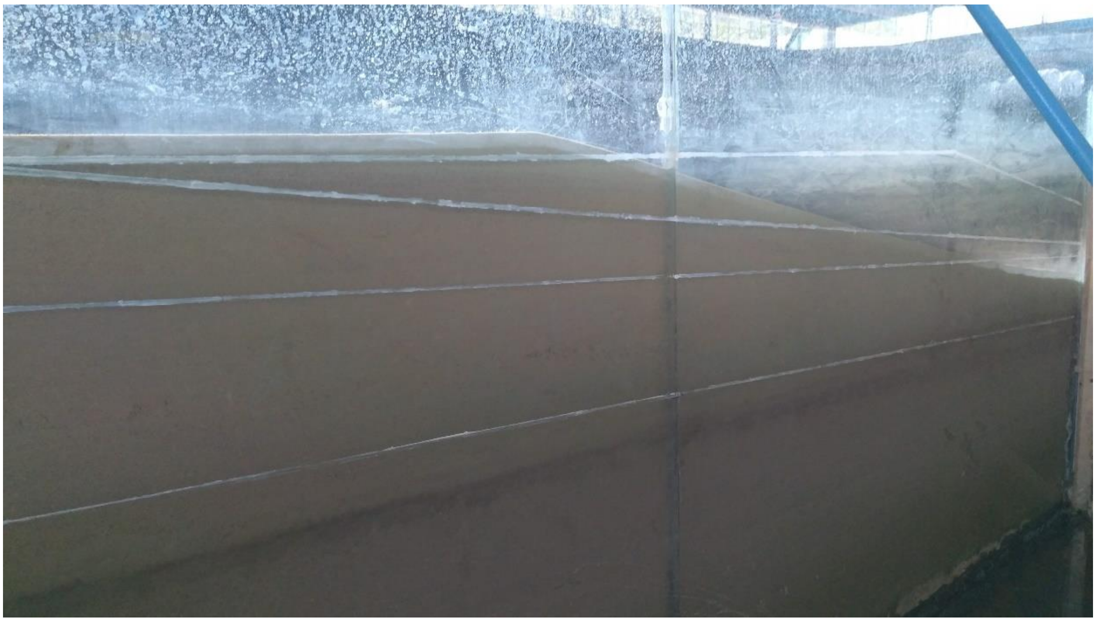

Figure A.12. Post-Storm Bottom Profile of Accretive Waves onto 1:10 Beach Fill

Figure A.13. Sand Berm and Bottom Profile of 1:10 Beach Fill after Accretive Waves

Figure A.14. Post-Storm Bottom Profile of Erosive Waves onto 1:10 Beach Fill

Figure A.15. Sand Bar Formation near Closure Depth under the Influence of Erosive Waves

Figure A.16. Post-Storm Bottom Profile of Accretive Waves onto 1:5 Beach Fill

Figure A.17. Sand Berm and Bottom Profile of 1:5 Beach Fill after Accretive Waves

Figure A.18. Acoustic Doppler Velocimetry Equipment

Figure A.19. Acoustic Doppler Velocimetry Setup

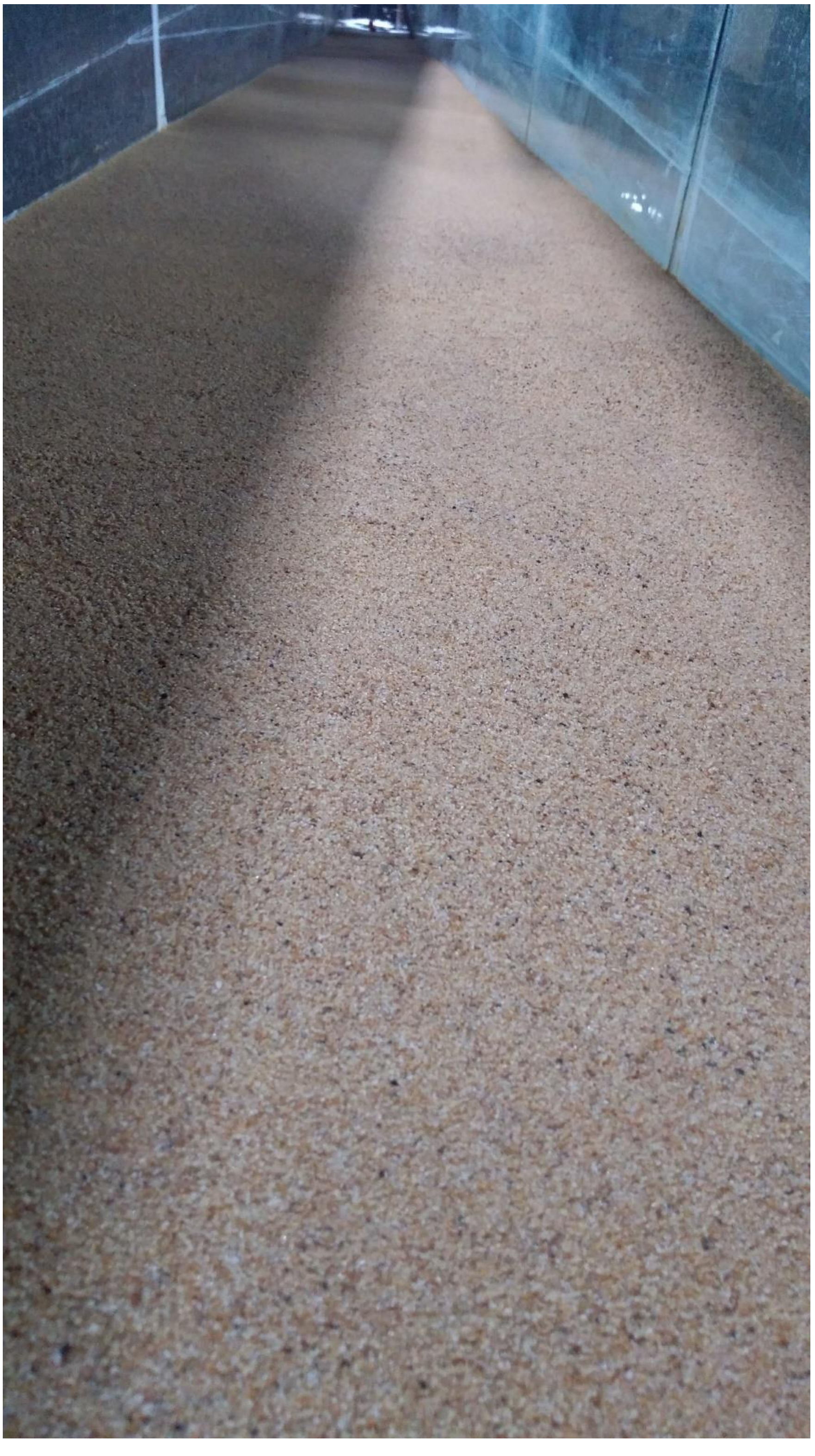

Figure A.20. Natural Beach Slope of 1:15 Consist of Coarse Sand

Figure A.21. Ripples Formed onto Coarse Sand Due to Erosive Waves

Figure A.22. Sand Bar Formation Due to Erosive Waves

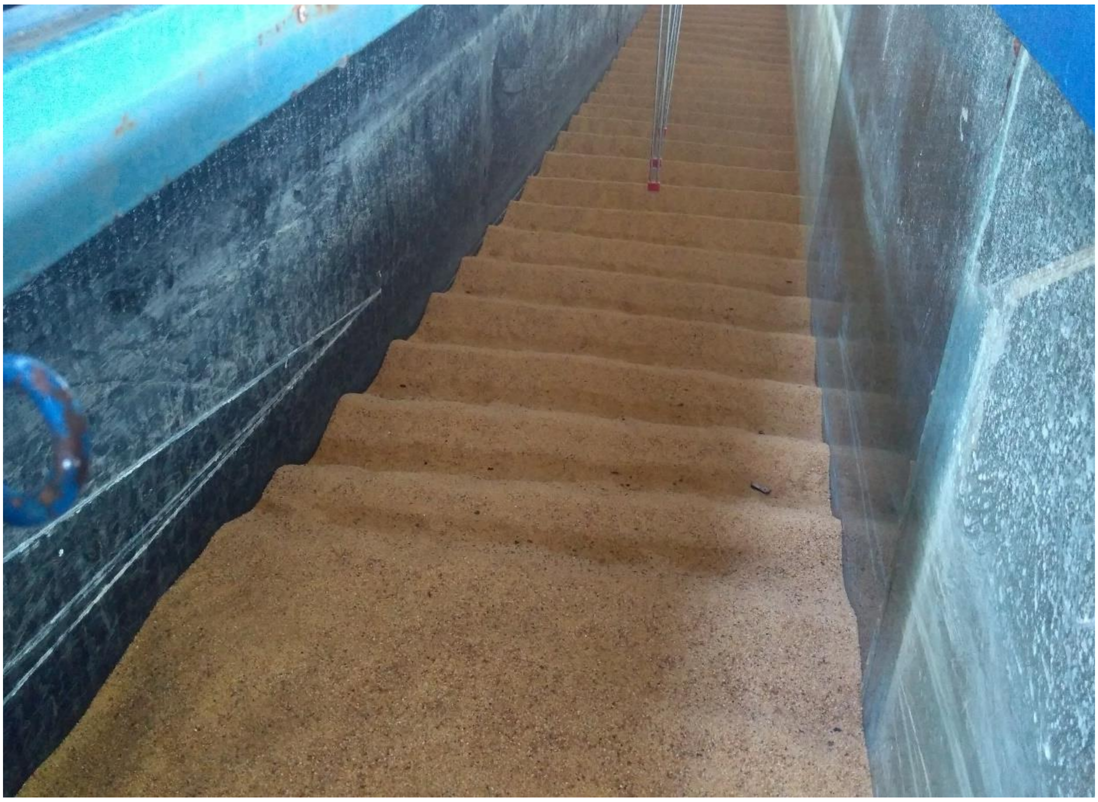

Figure A.23. Ripples Due to Erosive Waves

Figure A.24. Post-Storm Bottom Profile around Geotextile Tube After Accretive Waves

Figure A.25. Post-Storm Bottom Profile around Geotextile Tube After Erosive Waves

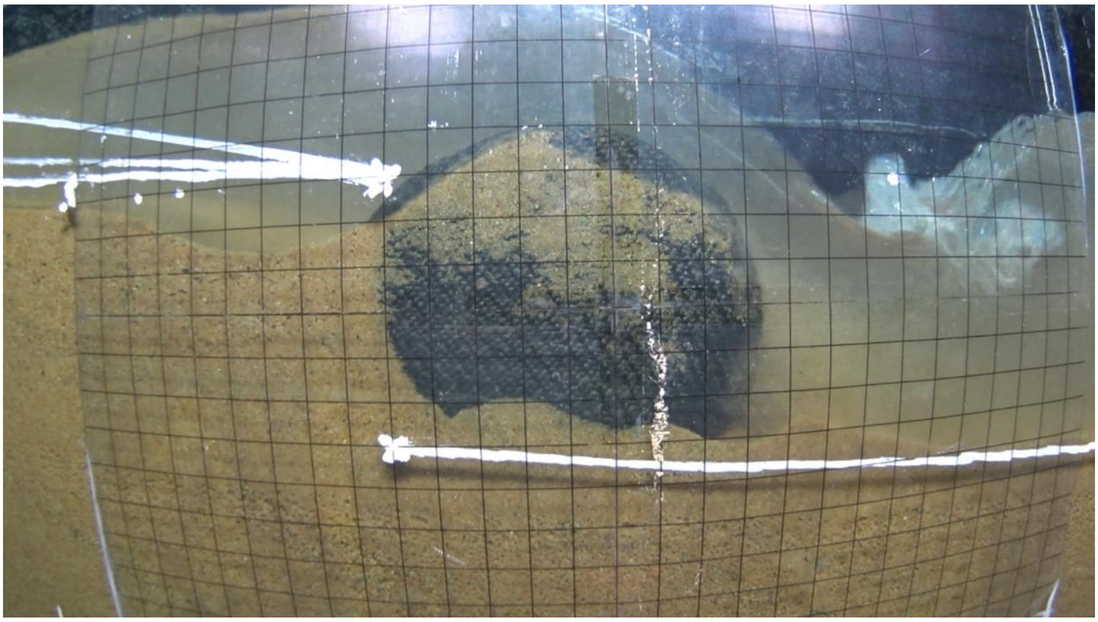

Figure A.26. Turbulence Observed around Geotextile Tubes

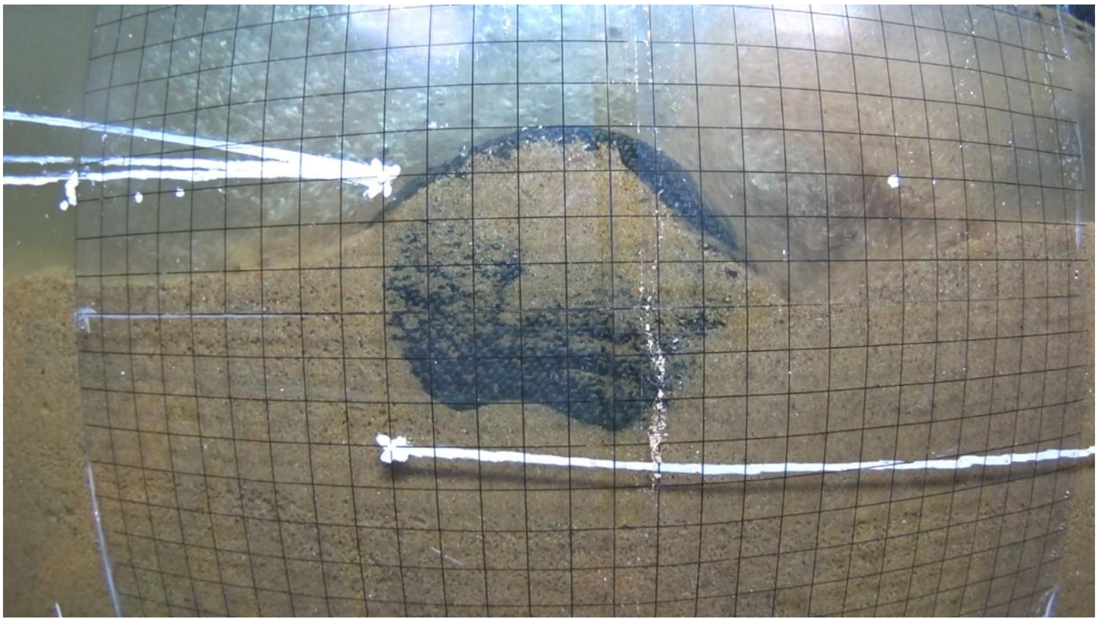

Figure A.27. Sediment Transport Observed around Geotextile Tubes